CHAPTER 4

THE ANALYSIS OF A CRACKED ROAD PAVEMENT

4.1 INTRODUCTION

The treatment of road-building materials with cement or lime has always been very popular because of the increased strength of the treated material. Both of these materials do however have the tendency to exhibit initial cracking soon after construction (Otte, 1976). For structural design purposes they should therefore be considered in the same way and a general term for both, treated material, will be used in this chapter.

The extent and width of the initial cracks in pavements with cement-treated bases were shown in Figure 3.1 (page 40). The author measured cracks of up to 10 mm wide in cement-treated crusher-run, but the width generally depends on the quality of the treated material and the position of the layer in the structural layout.

The effect and influence of initial cracks on the performance of pavements could, until recently, only be studied and evaluated by visual observation and speculation (Brewer and Williams, 1968; Otte, 1973a; George, 1974). It is difficult to quantify the effect of a crack since cracked layers are no longer continuous and the available computer programs, for example CHEVRON and BISTRO, are therefore really no longer suitable to do the analysis. This fact increased the complexity of the design of treated layers immensely, but a recent development in the finite element analysis technique may be one of the keys to the solution of the problem.

The objectives of this chapter, which includes a fair amount of detail, are (i) to indicate the application of finite element analysis to the study of a pavement containing a cracked treated layer, (ii) to make a tentative recommendation on the procedure that should be adopted to determine possible stress increases, (iii) to study previous applications of the finite element program to this problem, and (iv) to determine the extent of the stress increase in some of the typical layouts used in South Africa. To be able to follow and comprehend this chapter easily some understanding of finite element analysis is necessary, and it is assumed that the reader has this.

4.2 PRISMATIC SOLID FINITE ELEMENTS AND CRACKED TREATED LAYERS

4.2.1 The program

The finite element program used in this study was developed by Wilson and Pretorius (1970) and it employs constant strain prismatic solids. The latter were defined as three-dimensional solids which have constant two-dimensional geometric shapes and infinite third dimensions. The loading

into the third dimension is achieved by a Fourier series and this makes the program essentially three-dimensional.

Figure 4.1 explains some of the terminology, for example period length and loaded length, required to run the program. It should be noted that since the prismatic solids are continuous in the Z-direction, the crack can only occur in the YZ-plane. Some additional explanations of the program and information on the preparation of the input data are given in Appendix B.

4.2.2 Layout considered

It was decided to use only one structural layout to study the various ways of analysing a pavement containing a cracked treated layer. The chosen design is shown in Figure 4.2 but since the thin surfacing was considered to play only a minor role in the stress distribution, it was finally decided to analyse the structure shown in Figure 4.3.

The elastic moduli used for the various materials are given in Table 4.1 and a constant Poisson ratio of 0,35 was used for all the materials.

TABLE 4.1 : Elastic moduli of the materials considered in this analysis

MATERIAL	ELASTIC MODULUS (MPa)
Crusher-run	500
Treated layer	4 000
Subbase	500
Selected fill	200
Subgrade	100

4.2.3 Loading condition

The maximum legal wheel load in South Africa is 40 kN and a representative tyre contact pressure is 500 kPa. The prismatic solids program requires the load to be applied to a rectangular area, and an area of 270 x 296,3 mm was chosen. The CHEVRON program calculated the radius of the circular loaded area to be 157,81 mm.

4.2.4 Finite element representation

After careful planning and incorporation of the suggestions by Dehlen (1969) for the finite element representation of a pavement, it was decided to use the mesh shown in Figure 4.4. The total length of the section under consideration was taken as 9 000 mm with a height of 7 025 mm. The element sizes were chosen as shown, six elements underneath the load, six

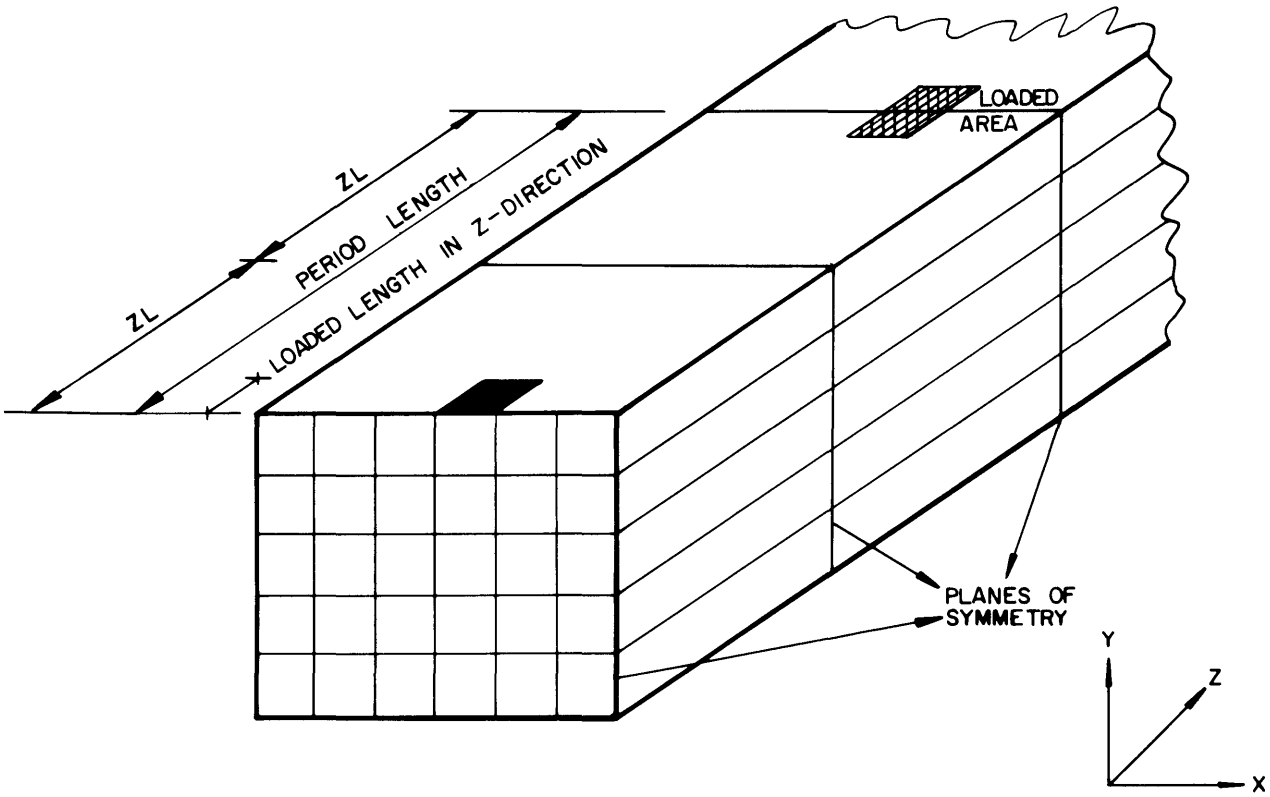

FIGURE 4-1

DEFINITION OF TERMINOLOGY REQUIRED TO RUN THE PRISMATIC SOLID FINITE ELEMENT PROGRAM.

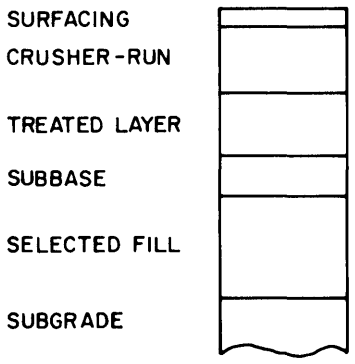

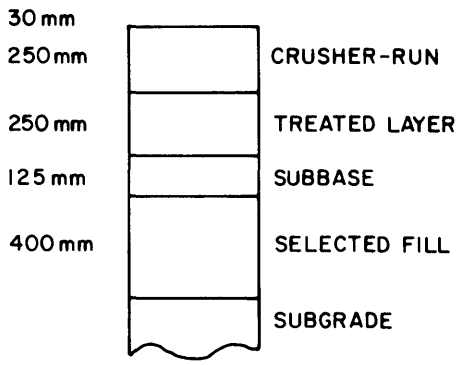

FIGURE 4-2 FIGURE 4-3

STRUCTURAL LAYOUTS CONSIDERED IN THE ANALYSIS OF A PAVEMENT CONTAINING A CRACKED TREATED LAYER

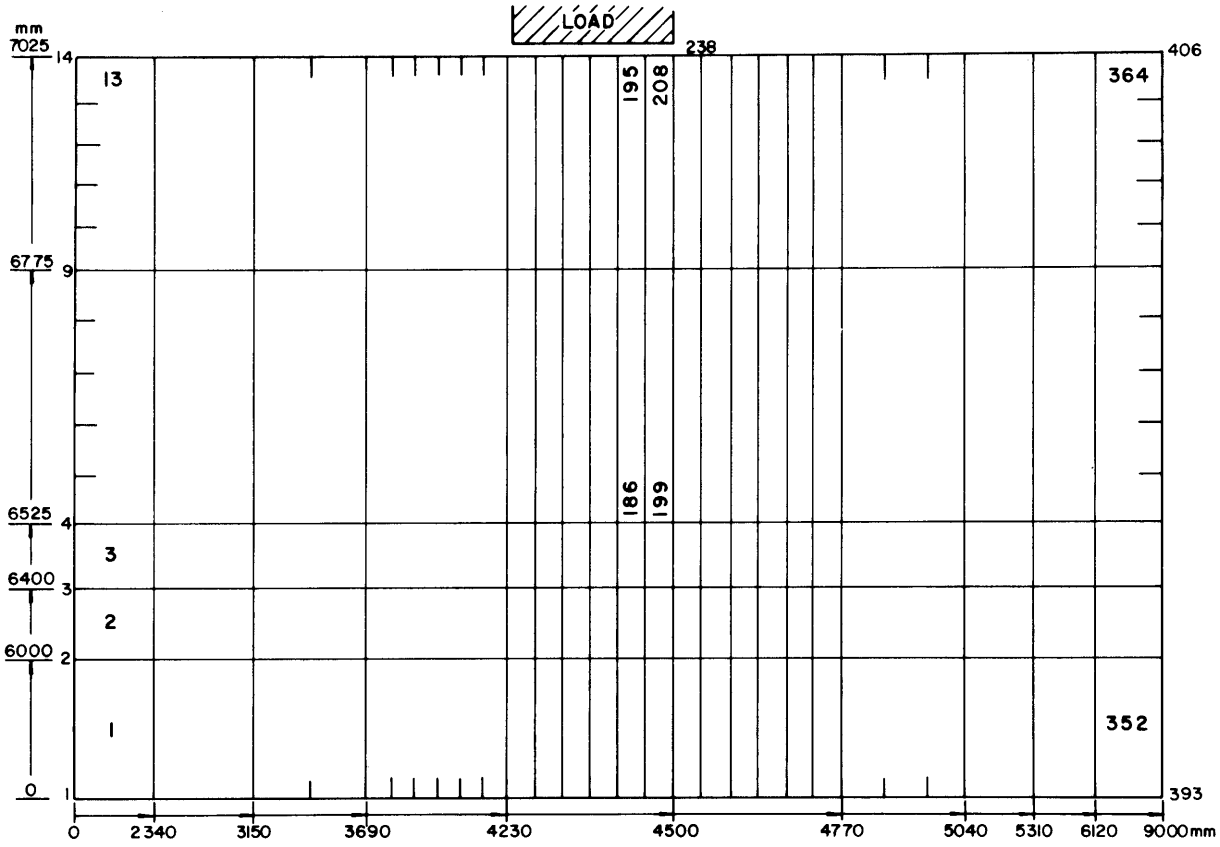

FIGURE 4-4

FINITE ELEMENT MESH - UNCRACKED CONDITION

elements in twice the loaded width (540 mm) on the left hand side of the loaded area and six in the loaded width (270 mm) on the right hand side of the load. The two upper layers were each divided into five 50 mm layers.

In another study (Otte, 1975) an axisymmetrical finite element program was used to analyse the mesh representing the uncracked pavement (Figure 4.4) and it was compared with a layered elastic theory analysis, namely CHEVRON. The differences in the stress values in the vicinity of the load were calculated to be about 7 per cent. This indicates that Figure 4.4 is an accurate and acceptable finite element representation of the pavement.

To run the prismatic solid finite element program it was necessary to make decisions on the following input requirements described in Appendix B.

(a) The nodal points along the two outer vertical boundaries were constrained to move only in the vertical direction (code = 1) whereas those along the bottom boundary were fixed (code = 3) and could not move at all. All the other nodal points were free to move in any direction.

(b) The load was applied at seven nodal points, two of 3 333,38 and five of 6 666,75 N. This resulted in a total load of very nearly 40 kN.

(c) The period length, which is the spacing in the Z-direction between the centres of two loads (Figure 4.1) was chosen after a CHEVRON analysis. The analysis showed that the surface deflection at 4 000 mm offset from the centre of the loaded area was only about 8 per cent of the maximum deflection and the horizontal tensile stress was less than 0,1 per cent of the maximum value. It was then decided to use a period length of 4 000 mm.

(d) The loaded length in the Z-direction was 148,15 mm and this indicated about 14 harmonics to represent the load. Only 11 harmonics were used with the 11th contributing less than 2 per cent to the maximum nodal point deflection (281 μm at nodal point 196).

4.2.5 Analysis of a pavement containing a cracked treated layer

To model a pavement containing a cracked treated layer the finite element mesh shown in Figure 4.5 was used. This mesh will hereafter be referred to as Case A. It was necessary to spend some time in determining the optimum procedure for numbering the nodal points in order not to exceed the specification on the maximum difference between nodal points defining an element (see Appendix B). The procedure that was accepted can be obtained from the nodal point numbers given in Figure 4.5.

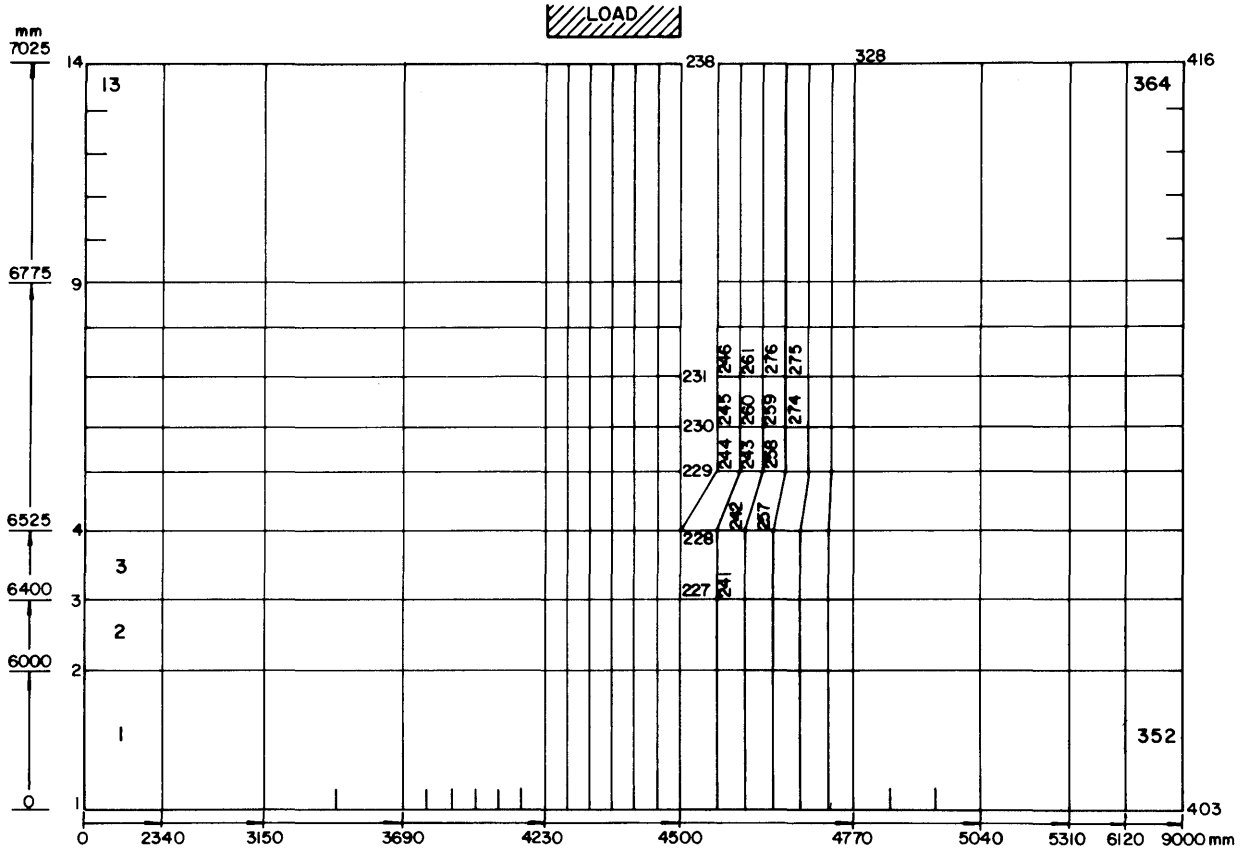

FIGURE 4-5

FINITE ELEMENT MESH - CASE A

The crack width was assumed to be 6 mm which represents a wide crack with no load transfer across it. The crack spacing was assumed to be 4 500 mm, which agrees with practical observations (Otte, 1973a).

The lower four nodal points on each of the two outer vertical boundaries were constrained and could move only in the vertical direction. The other (that is, the upper) nodal points on the outer vertical boundaries were allowed to move freely since they formed the edges of other cracks. The nodal points along the sides of the crack were allowed to move in any direction but those along the bottom boundary of the mesh were fixed and could not move at all (see Appendix B).

In a previous study (Otte, 1975) the stresses parallel to the crack (σ_{zz})* and those perpendicular to the crack (σ_{xx}) in both the cracked (Case A) and uncracked conditions were compared at various offsets from the centre of the load. It was observed that (i) the maximum tensile stress in the treated layer occurred at the bottom of the layer; (ii) the σ_{xx} stress was not significantly affected by the introduction of the crack, it decreased by 20 per cent; (iii) the direction of the maximum tensile stress changed from being perpendicular to the crack (in the X-direction) to parallel to the crack (in the Z-direction); (iv) the σ_{zz} stress increased significantly so that it exceeded the maximum tensile σ_{xx} by about 80 per cent, and (v) a more accurate comparison of the maximum stresses may be possible if the maximum values could be obtained from accurately prepared stress contour maps since the position of the maximum stress will probably not coincide with the centre point of one of the elements.

From observations (i), (iii) and (iv) in the previous paragraph it was concluded that the maximum horizontal tensile stress in a cracked cement-treated layer will occur at the bottom of the cement-treated layer and it will act parallel to the crack (σ_{zz}). This agrees with the conclusions by Pretorius (1970).

4.2.5.1 An alternative method (L-model)

A large vertical tensile stress at the bottom and next to the crack, but on the opposite side of the load, was observed during the analysis of Case A. This large vertical stress may result in a loss of bond between the treated layer and the subbase, and the formation of a horizontal crack between these two layers. A pavement containing a cracked treated layer should therefore really be modelled by including the narrow horizontal

---

* σ_{zz} is a normal stress parallel to the z-axis which acts on a plane perpendicular to the z-axis.

crack between the two layers. If this is done the material above the horizontal crack and to the right of the vertical crack shown in Figure 4.5 may be eliminated from the model since there is no structural continuity between the layers. This suggested the finite element model shown in Figure 4.6. It will hereafter be called the L-model. This type of model was also used by Pretorius (1970) although a much finer, and hence possibly a more accurate mesh, was used in this study.

The maximum tensile stress in Case A was about 224 kPa and in the L-model it was calculated as 199 kPa. The small difference in tensile stress and the high vertical tensile stress next to the crack in Case A (Figure 4.5) prompted the suggestion that the L-model should be used. Additional advantages of the L-model are that it is easier to change the depth of the crack (see later) and that the computer time is about 35 per cent less than that for the Case A analysis. The CPU time to analyse the L-model on an IBM S 370/158 computer running under OS R21,8 was about 14 minutes.

4.2.5.2 A third alternative method

It is also possible to analyse a pavement containing a cracked treated layer by applying the principle of axisymmetrical and asymmetrical loading. Figure 4.7 is a schematic drawing explaining the principle, namely that a one-unit load next to the vertical crack may be represented by an axisymmetrical load of 0,5 units and an asymmetrical load of 0,5 units. Two analyses are performed, one for the axisymmetrical load and another for the asymmetrical load, each having a load of 0,5 units. When the calculated stresses are added together the outcome is the stress when a one-unit load is placed next to the crack. By doing it this way the principle of superposition is assumed, which implies that the two 0,5 unit loads on the left hand side of the crack cancel out and the two on the right hand side produce a one-unit load next to the crack.

Figure 4.8 shows the boundary conditions that were used, namely the nodal points on the vertical cracked faces were allowed to move freely (code = 0); those on the bottom boundary were fully constrained (code = 3); the nodal points on the lower outer vertical edges for the axisymmetrical load were allowed to move only vertically and for the asymmetrical load they were allowed to move only horizontally (see Appendix B). The mesh layout and the element sizes were the same as used in Figure 4.4.

A detailed comparison between the stresses calculated for this loading condition and those of Case A (Figure 4.5) has been done elsewhere

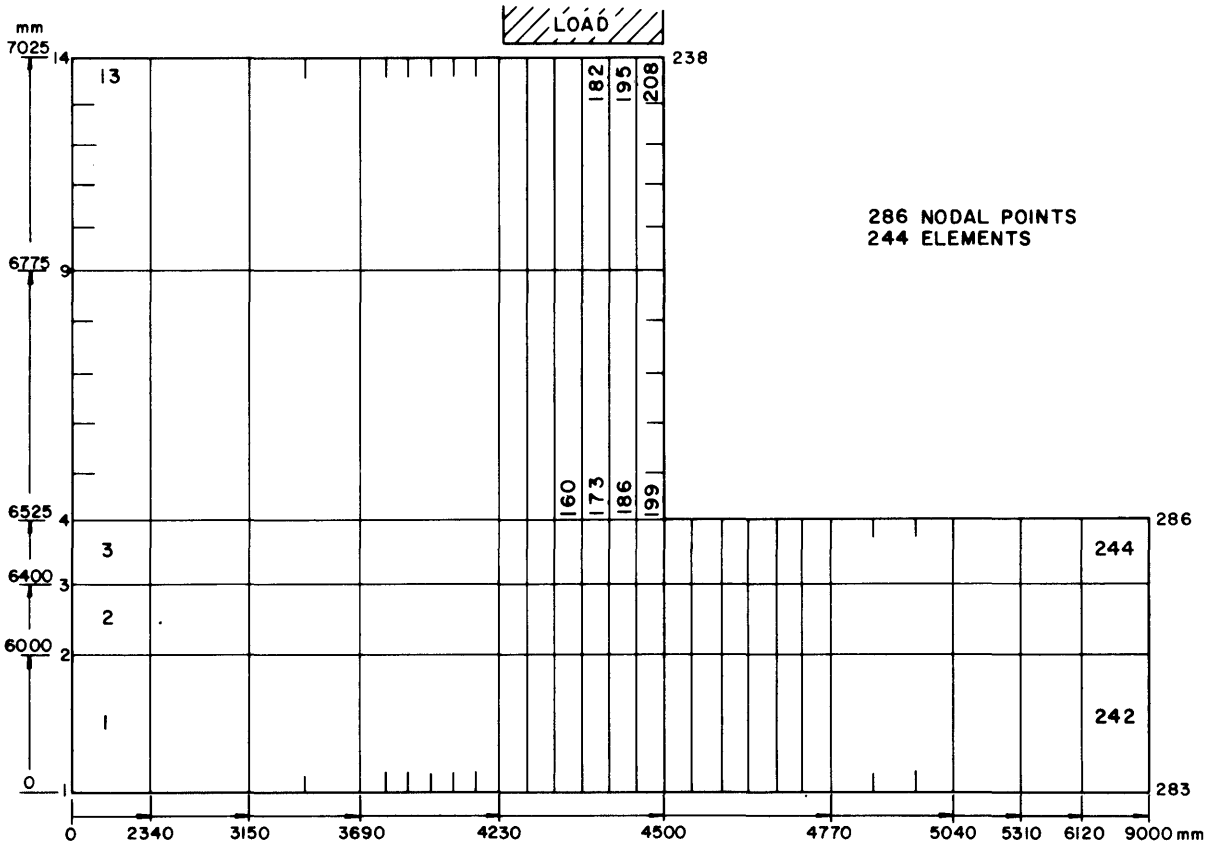

FIGURE 4-6

FINITE ELEMENT MESH OF L-MODEL

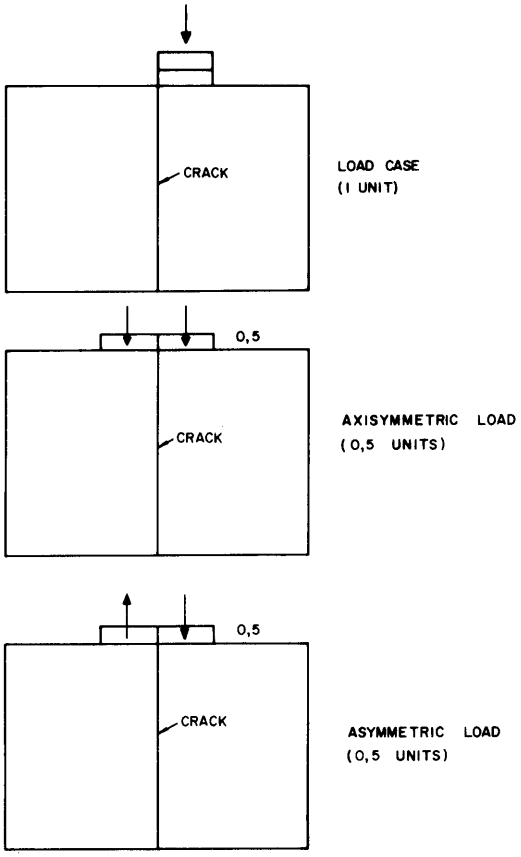

A LOAD OF 1 UNIT NEXT TO THE VERTICAL CRACK IS EQUAL TO AN AXISYMMETRICAL LOAD OF 0,5 UNITS PLUS AN ASYMMETRICAL LOAD OF 0,5 UNITS

FIGURE 4-7
LOADING PRINCIPLE FOR ANALYSIS OF A PAVEMENT CONTAINING A CRACKED TREATED LAYER

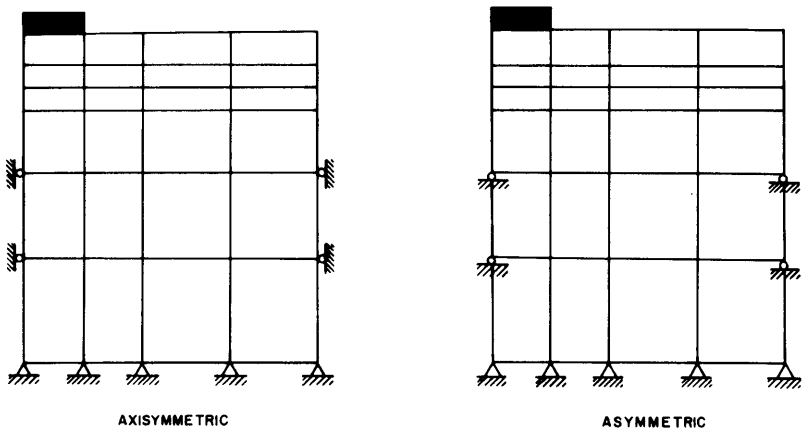

FIGURE 4-8
BOUNDARY CONDITIONS FOR AXISYMMETRIC AND ASYMMETRIC LOADS

(Otte, 1975). It was observed that the differences in stress near the crack were usually below 10 per cent but in some of the outlaying elements with low stress values the difference increased to around 50 per cent with a maximum difference of 170 per cent. The difference between the maximum stresses calculated for the two conditions was only 8 per cent, and this was considered very acceptable. Assuming the model in Figure 4.5 (Case A) to be 'correct', it may be concluded that loading next to the edge of a vertical crack may be represented by the sum of an axisymmetrical and asymmetrical analysis, each with half of the load intensity.

It therefore seems that both the L-model and the axisymmetrical plus asymmetrical loading may be used to analyse a pavement containing a cracked treated layer. Otte (1975) compared the stresses calculated by these two methods at the bottom of the treated layer. The agreement in the σ_{xx} values was generally very poor while the differences in the σ_{yy} and σ_{zz} values were generally about 10 per cent. Since the maximum horizontal tensile stress always seems to be a σ_{zz} value, either of the two analysis methods may be accepted. There are also other factors to be considered, such as computer time and the manual labour involved in summing the outcome of the axisymmetrical and asymmetrical loadings. It is therefore suggested that the L-model should be used in preference to this loading method to represent a pavement containing a cracked treated layer, and it will be used in the remainder of this chapter.

4.2.6 Increase in tensile stress

The increase in maximum horizontal tensile stress caused by the crack can be defined and calculated as the difference between the maximum stress obtained from the appropriate finite element model and the maximum calculated by a CHEVRON analysis. To determine the maximum stress from the finite element models, stress contour maps were prepared (Otte, 1975). This was found to be very time-consuming and the development of an easier alternative was very desirable.

Further analyses indicated that the most convenient way to determine the increase in horizontal tensile stress caused by the crack would be to do a finite element analysis of the L-model and to locate the maximum horizontal tensile stress. It is usually a σ_{zz} value in the centre of a finite element at the bottom of the treated layer. The next step is to record σ_{zz} in the centre of the finite element directly above the finite element containing the maximum σ_{zz}, and it will generally have a lower value. The stress gradient between these two points should then be projected

downwards to calculate the maximum stress (σ_{mc}) at the bottom of the treated layer. It is suggested that this value (σ_{mc}) should be taken as the maximum σ_{zz} in the treated layer. A CHEVRON analysis should hereafter be performed to calculate the maximum tensile stress for the uncracked case (σ_{mu}). The increase in maximum horizontal tensile stress as a result of the crack is then expressed as the difference between the two stress values, that is $\sigma_{mc}-\sigma_{mu}$.

To illustrate the previous suggestion, the maximum tensile stress for a pavement containing a cracked treated layer (hereafter referred to as the cracked condition) was calculated. The maximum σ_{zz} occurred at the centre of element 173 (Figure 4.6) and was 199 kPa. The σ_{zz} at the centre of element 174 was 105 kPa. The two centres are 50 mm apart and this resulted in a stress gradient of 1,88 kPa per mm. The bottom of the layer is 25 mm below the centre of element 173 resulting in a stress of 199 + (1,88 x 25) = 246 kPa (σ_{mc}). The stress contour map (Otte, 1975) indicated a maximum value of about 250 kPa, and this agrees very reasonably with the suggested method.

A CHEVRON analysis of the uncracked pavement indicated the maximum horizontal tensile stress (σ_{mu}) to be about 213 kPa and it occurred underneath the centre of the wheel. The stress increase, as a result of the crack, is therefore about 33 kPa, from 213 to 246 kPa, and that is an increase of about 15 per cent.

It can happen that a steeper stress gradient may occur between some of the adjoining elements, and coupled with the particular stress values, this may result in a larger stress increase. Although these exceptions do not occur very frequently, it is essential that the analyser should also investigate the stress gradients in the surrounding elements during his search for the maximum stress.

If the suggestion of calculating the maximum horizontal tensile stress (σ_{mc}) is adopted, it is not necessary to prepare the stress contour map although the principle of its preparation is used. It is also implicitly assumed that the maximum stress will occur directly beneath the centre of the finite element having the maximum σ_{zz} value, and, based on the previous analyses, it is believed that this is a valid assumption.

4.2.7 Surface deflection

Figure 4.9 shows the surface deflection calculated by three finite element models. The uncracked pavement (Figure 4.4) produced a fairly symmetrical deflection pattern with the maximum value occurring underneath the centre

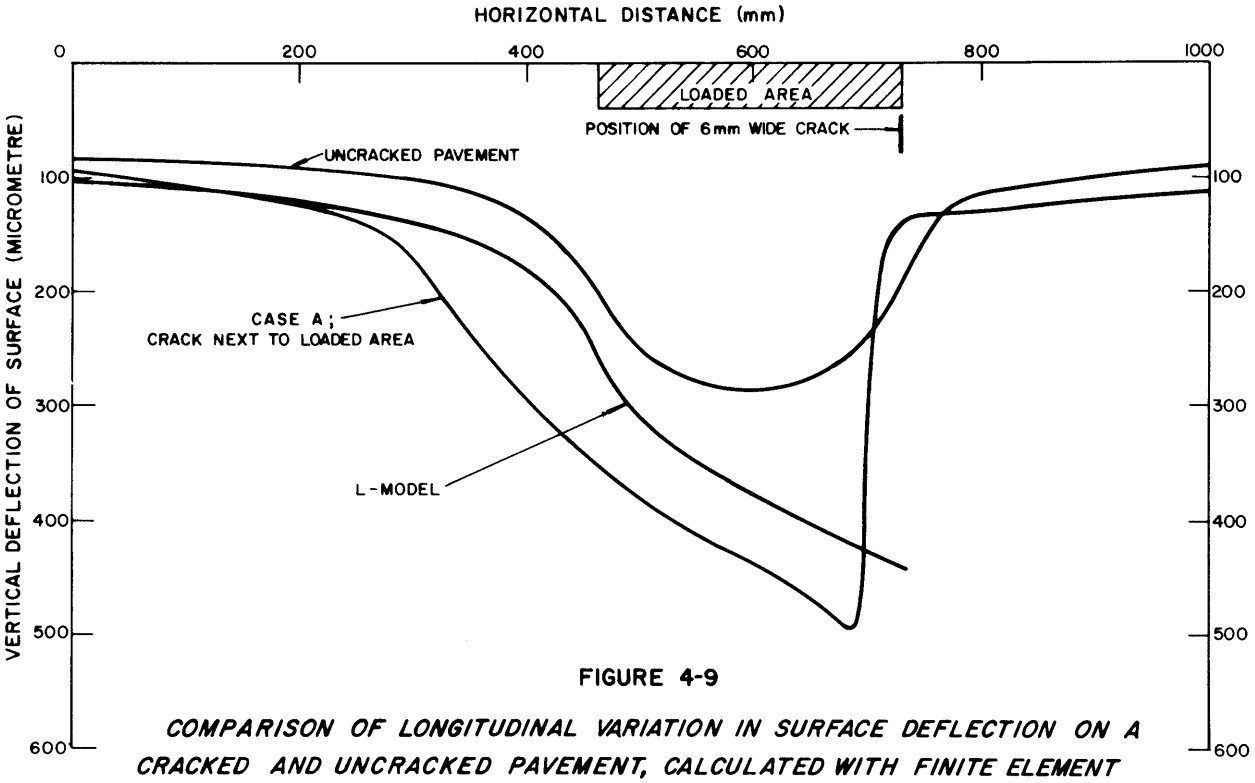

FIGURE 4-9

COMPARISON OF LONGITUDINAL VARIATION IN SURFACE DEFLECTION ON A CRACKED AND UNCRACKED PAVEMENT, CALCULATED WITH FINITE ELEMENT ANALYSIS

of the loaded area. The patterns for Case A and the L-model are very similar with a slight difference in the absolute value.

The variation in deflection across the crack is quite interesting. Although a wide crack was assumed in Case A, and no load transfer was supposed to take place across it, the unloaded right hand side deflected about 140 micrometres. This means that some load transfer did take place; probably through the subbase and subgrade in the form of the high vertical tensile stresses which occurred to the right of the crack and at the bottom of the treated layer (see 4.2.5.1, page 59). The amount of load transfer which does take place in Case A is another reason why the L-model (Figure 4.6) should preferably be used.

4.2.8 Vertical stress in the subgrade

If a wide crack is formed in a treated layer the loss of horizontal load transfer across the crack may result in a significant increase in vertical compressive stress in the lower-lying materials next to the crack (Fossberg et al, 1972a). This may cause deformation of the subgrade next to the crack which may lead to an unacceptable riding quality on the road. In the design of a pavement containing a cracked treated layer it may therefore be important to take due notice of the increase in vertical compressive stress and the possibility that deformation may develop. The prismatic solids finite element program was also used to investigate this phenomenon (Otte, 1975) and it was observed that the possibility of subgrade deformation after cracking, and next to the crack in some structural layouts, may not be disregarded (see later).

4.3 STRESS DISTRIBUTION IN CRACKED TREATED LAYERS

4.3.1 Previous use of program

The prismatic solids finite element program was previously used by Pretorius (1970) to study the fatigue behaviour of a cement-treated layer. Recently Luther et al (1974) studied reflection cracking through bituminous overlays with the aid of this program.

Pretorius (1970) analysed the pavement shown in Figure 4.10 using the finite element mesh shown in Figure 4.11. The wheel load was assumed to be two 20 kN loads, applied to two square areas of 203 x 203 mm (8 inches by 8 inches) and the centres were 304,8 mm (12 inches) apart. To obtain the maximum stress between the two loads of the 40 kN dual wheel, he calculated the stress parallel to the crack at Z=152,4 mm (Appendix B) under a 20 kN load, and doubled it. This value was compared with the results of a

ASPHALTIC CONCRETE	E = 4000 MPa υ = 0,35	d = 75 mm
CEMENT-TREATED BASE	E = 19300 υ = 0,16	d = 200 mm
FOUNDATION	E = 69 AND 11 υ = 0,45	

FIGURE 4-10

PAVEMENT ANALYSED BY PRETORIUS (1970)

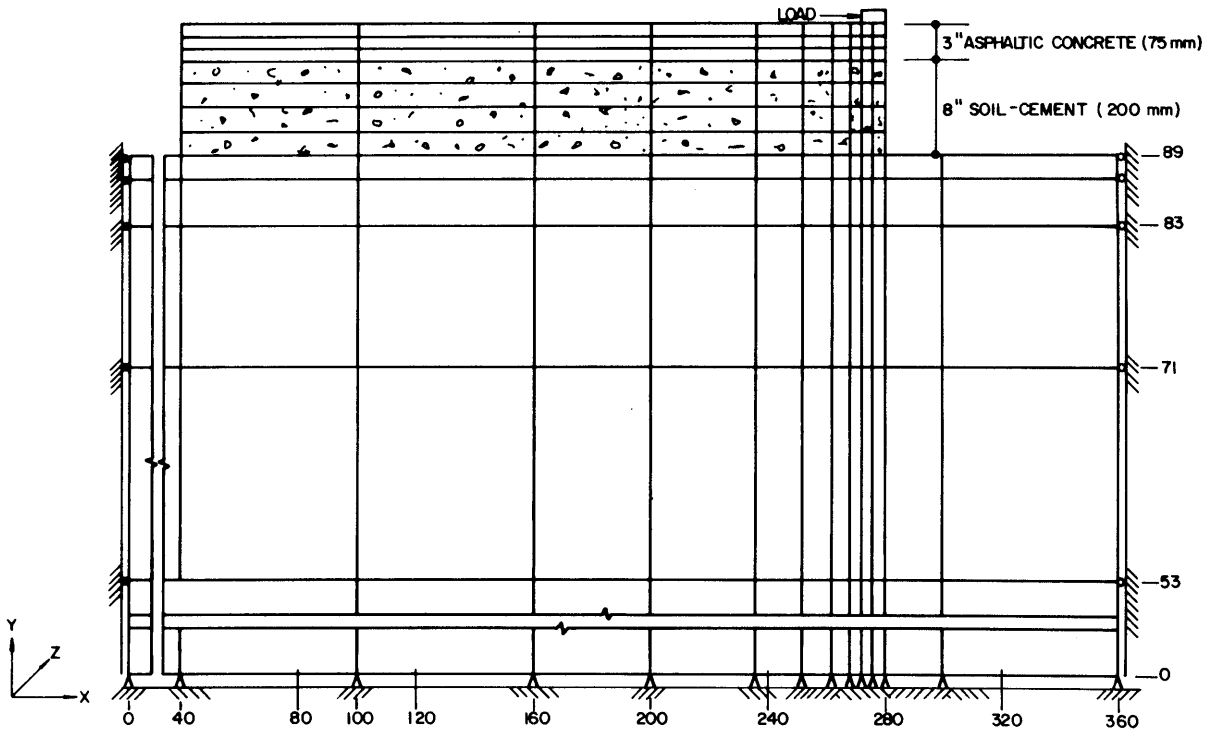

NOTE : DIMENSIONS ARE IN INCHES

FIGURE 4-11

FINITE ELEMENT MESH FOR LOAD AT AN EDGE (After Pretorius, 1970)

CHEVRON analysis and it was possible to calculate the stress increase. The increase in horizontal tensile stress caused by the crack was calculated as about 46 per cent on the 69 MPa subgrade and as about 60 per cent on the 11 MPa subgrade (Mitchell et al, 1974).

The mesh shown in Figure 4.11 was analysed by the author and the maximum tensile stress between the wheels (on a 69 MPa subgrade) was calculated as 1 022 kPa. The CHEVRON analysis indicated a stress of 770 kPa and hence a 33 per cent stress increase. The corresponding figures reported by Pretorius (1970) were about 758 and 517 kPa which resulted in the increase of about 46 per cent mentioned above. The stress increase calculated by the author was less than that calculated by Pretorius. The discrepancy in the calculated stress values may be due to some small differences, for example in the loading conditions.

The finite element mesh shown in Figure 4.12 was used to analyse the structure shown in Figure 4.10 in an effort to determine the effect of the mesh size. A 69 MPa subgrade was used. The loading system was changed to that described in section 4.2.4; hence one 40 kN load on a 270 x 296,3 mm area was used. It was considered acceptable to make this change in the loading condition since CHEVRON indicates that the maximum tensile stress would increase by about 9 per cent when the loading is changed from two 20 kN loads to one 40 kN load. The maximum horizontal tensile stress in the finite element analysis occurred at the bottom of element 189 and was 1 306 kPa. The CHEVRON analysis with a corresponding loading system indicated a maximum tensile stress of 840 kPa and the stress increase because of the crack was 55 per cent.

From the foregoing it seems that the refinement in the mesh (Figure 4.11 to 4.12) resulted in a 28 per cent increase in the calculated maximum tensile stress - from 1 022 to 1 306 kPa. Using the finer, and probably more accurate, mesh is therefore significant.

4.3.2 Layouts considered

It was the intention to study several typical structural layouts to obtain the percentage increase in stress. There is, however, such a multitude of possible combinations with respect to layer thickness and elastic properties that only two basic structural sections were chosen, namely one with and one without a crusher-run base. The bituminous surfacing was omitted in all the analyses. From this multitude of possible layouts eight were selected and analysed. In some of them the elastic moduli of the treated layers were varied while the properties of the other layers were

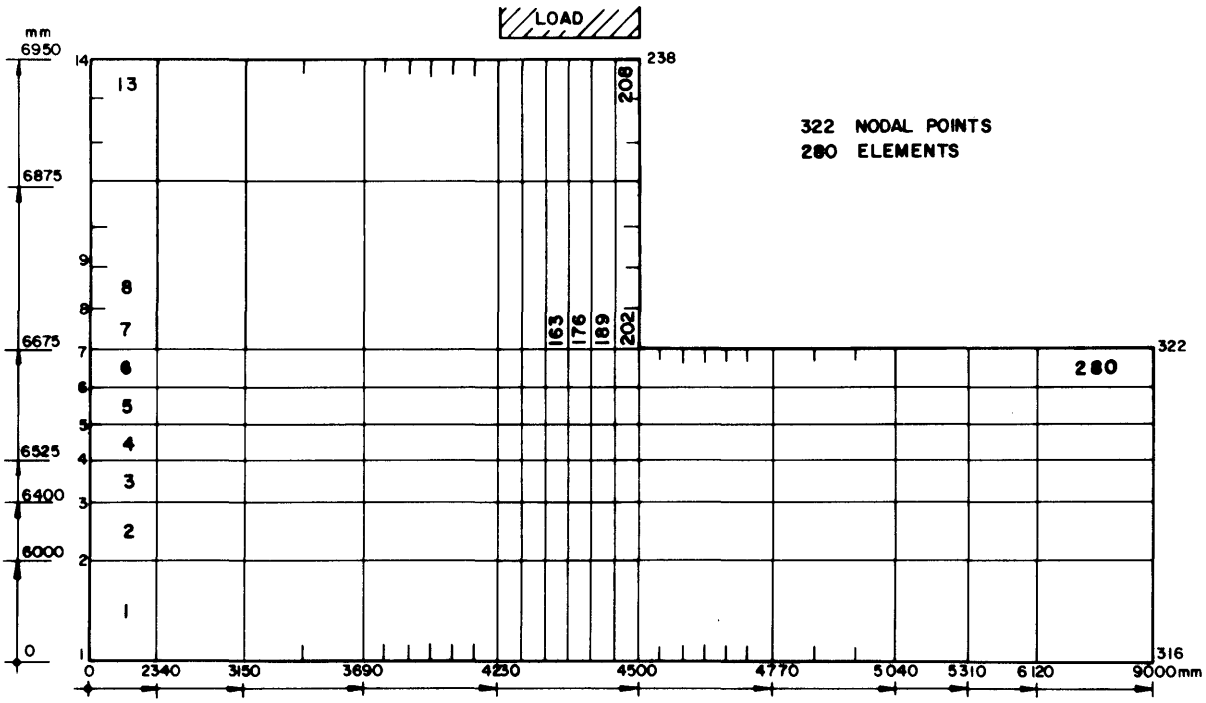

FIGURE 4-12

IMPROVED FINITE ELEMENT MESH

kept constant. A constant Poisson ratio of 0,35 was assumed for all the materials.

Figure 4.13 illustrates the selected thicknesses, elastic moduli and material types in the various layouts. The depth of the crack considered in each analysis is shown by the jagged vertical line. The thicknesses were based on South African experience and the moduli were obtained from published literature. Layouts A to C are typical of the designs used in the Transvaal where an untreated crusher-run layer is used on top of, usually, a cement-treated subbase (Otte and Monismith, 1976). In layout D a cement-treated crusher-run base was included between the treated and untreated layer. Layout E contains two treated layers, either cement or lime, while the upper treated layer in layout F will usually be a cement-treated crusher-run layer. Layout G was used on two roads during the sixties (Special Road S12 and a part of Route N4) but their performances were not entirely satisfactory (Otte, 1973a). Layout H is essentially the same as G but with thicker layers. Both have an untreated layer between two treated layers.

4.3.3 Results

The finite element model shown in Figures 4.6 and 4.12 (L-model) was adopted and modified to accommodate the changes in the depth of the crack. It was analysed 21 times to cover the combinations shown in Figure 4.13. The method described in section 4.2.6 was used to calculate the maximum horizontal tensile and vertical compressive stresses in the cracked pavement.

4.3.3.1 Tensile stress in treated layers

In all cases the maximum tensile stress occurred at the bottom of the treated layer and it acted parallel to the crack. This confirms the observation by Pretorius (1970). The maximum stress usually occurred between the centre of the loaded area and the crack, whilst it always occurred directly beneath the centre of the loaded area in CHEVRON. Tables 4.2 and 4.3 contain the maximum stresses as recorded for the eight layouts; they show the increase in maximum horizontal tensile stress at the bottom of the treated layer and the surface deflection according to CHEVRON.

It seems that the maximum increase in tensile stress (39,3 per cent) as a result of the crack occurred in the treated base of layout D (Table 4.3) while a stress decrease was noticed in layouts A and H. Another interesting observation is the relatively high stress increases in layouts with thick (250 to 300 mm) upper layers in relation to the small increases in layouts

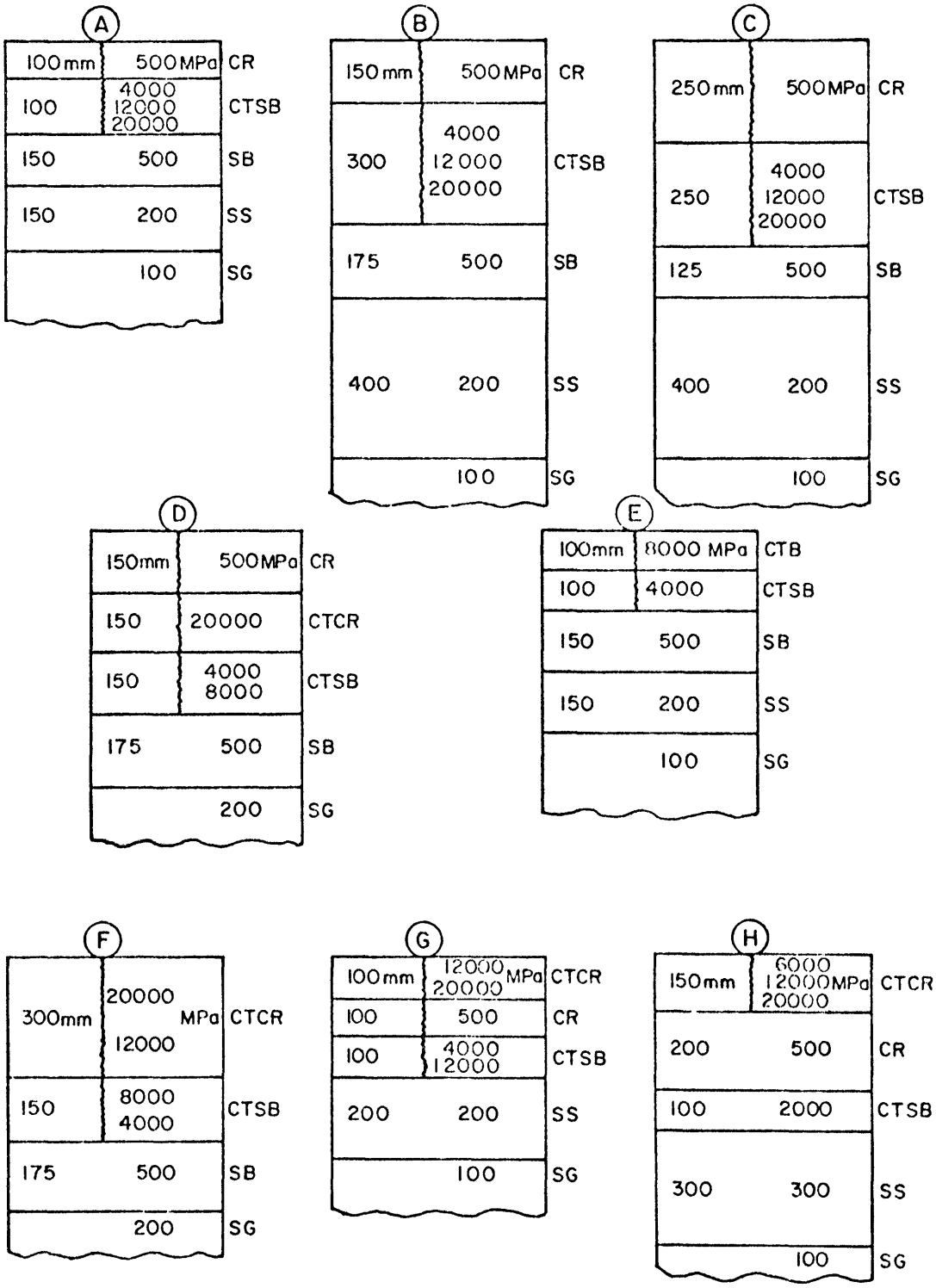

CR = CRUSHER-RUN BASE
CTCR = CEMENT-TREATED CRUSHER-RUN BASE
SB = SUBBASE
SS = SELECTED SUBGRADE
SG = SUBGRADE
CTSB = CEMENT-TREATED SUBBASE
CTB = CEMENT-TREATED BASE
(THE VERTICAL LINE IN EACH LAYOUT SHOWS THE DEPTH OF THE CRACK)

FIGURE 4-13
SCHEMATIC DRAWING OF ANALYSED LAYOUTS

TABLE 4.2 : Maximum horizontal tensile stresses in cracked and uncracked pavements

LAYOUT	ELASTIC MODULUS OF TREATED LAYER (MPa)	MAXIMUM HORIZONTAL TENSILE STRESS IN TREATED LAYER (kPa)		PERCENTAGE INCREASE IN TENSILE STRESS DUE TO CRACK	SURFACE DEFLECTION FROM CHEVRON (μm)
		Finite element analysis (cracked pavement)	CHEVRON program (uncracked)		
A	4 000	595	658	-9,6	394
	12 000	1 418	1 438	-1,3	356
	20 000	1 964	1 903	3,2	335
B	4 000	254	217	17,1	273
	12 000	476	364	30,8	240
	20 000	587	430	36,5	227
C	4 000	254	213	19,2	322
	12 000	509	382	33,2	298
	20 000	644	466	38,2	288

TABLE 4.3 : Maximum horizontal tensile stresses in cracked and uncracked pavements

LAY-OUT	ELASTIC MODULUS (MPa)		MAXIMUM HORIZONTAL TENSILE STRESS IN TREATED LAYER (kPa)				PERCENTAGE INCREASE IN STRESS DUE TO CRACKS		SURFACE DEFLEC-TION BY CHEVRON (μm)
			Base		Subbase				
	Base	Sub-base	Finite element analysis (cracked)	CHEVRON (un-cracked)	Finite element analysis (cracked)	CHEVRON (un-cracked)	Base	Sub-base	
D	20 000	4 000	596	447	199	161	33,3	23,6	203
	20 000	8 000	333	239	337	256	39,3	31,6	194
E	8 000	4 000	In compression		514	513	-	0,2	248
F	20 000	8 000	289	225	202	153	28,4	32,0	69
	12 000	4 000	290	232	142	113	25,0	25,7	82
G	12 000	4 000	1 570	1 352	489	411	16,1	19,0	258
	12 000	12 000	1 430	1 214	933	805	17,8	15,9	237
	20 000	4 000	2 147	1 829	412	351	17,4	17,4	238
	20 000	12 000	1 967	1 657	820	697	18,7	17,6	219
H	6 000	2 000	675	719	-	-	-6,1	-	221
	12 000	2 000	1 008	1 042	-	-	-3,3	-	194
	20 000	2 000	1 271	1 294	-	-	-1,8	-	176

A and E which had thin (100 mm) upper layers. This observation did not quite fit Layout G, but since this design and layout H should preferably not be used in pavement design (see 2.2.4, page 16) very little attention will be paid to them in the remaining part of the chapter. They were mainly analysed as part of an ongoing study to evaluate their previously unacceptable performance (Otte, 1973a). In both of them the increase in stress due to the cracks was less than 20 per cent, which is not considered to be excessive.

The possible existence of a relationship between the increase in tensile stress due to cracks and the thickness of the upper layers led to the preparation of Figure 4.14. Area A represents layouts A to D, that is those with an untreated base, while area B represents layouts E and F. No sound statistical relationship could be computed between the variables, but the figure may be used to obtain an indication of the expected increase in maximum horizontal tensile stress due to cracks once the surface deflection has been calculated.

4.3.3.2 Vertical compressive stress in lower layers

Table 4.4 shows the vertical stresses and strains in the two untreated layers underlying the cracked treated layer. In some of the layouts, for example A, B, C and E, they are the subbase and selected subgrade and, in others, for example D and F, they are the subbase and subgrade. These values were calculated by finite element analysis (for the cracked pavement) and CHEVRON (for the uncracked pavement). The strain for the finite element analysis was calculated by increasing the strain obtained from the CHEVRON analysis by the same ratio as the increase calculated for the corresponding vertical stresses.

The table shows that the increase in vertical stress due to cracking is dependent on the layout and that it is significant - the increase varies between about 2 and 15 times. For subgrade-quality materials Dormon and Metcalf (1965) have suggested a vertical strain below 650 με to withstand about one million load repetitions. Assuming this order of strain to hold also for both subbase and selected subgrade-quality materials, it seems that the strains in the first layer below the cement-treated layer of layouts A, E and G, when cracked, are rather excessive and deformation will probably occur before a million load repetitions. The other layouts may withstand one million load repetitions without severe rutting and deformation next to the crack, but the strains are approaching the allowable limit, and should water penetrate into the lower layers, severe deformation will

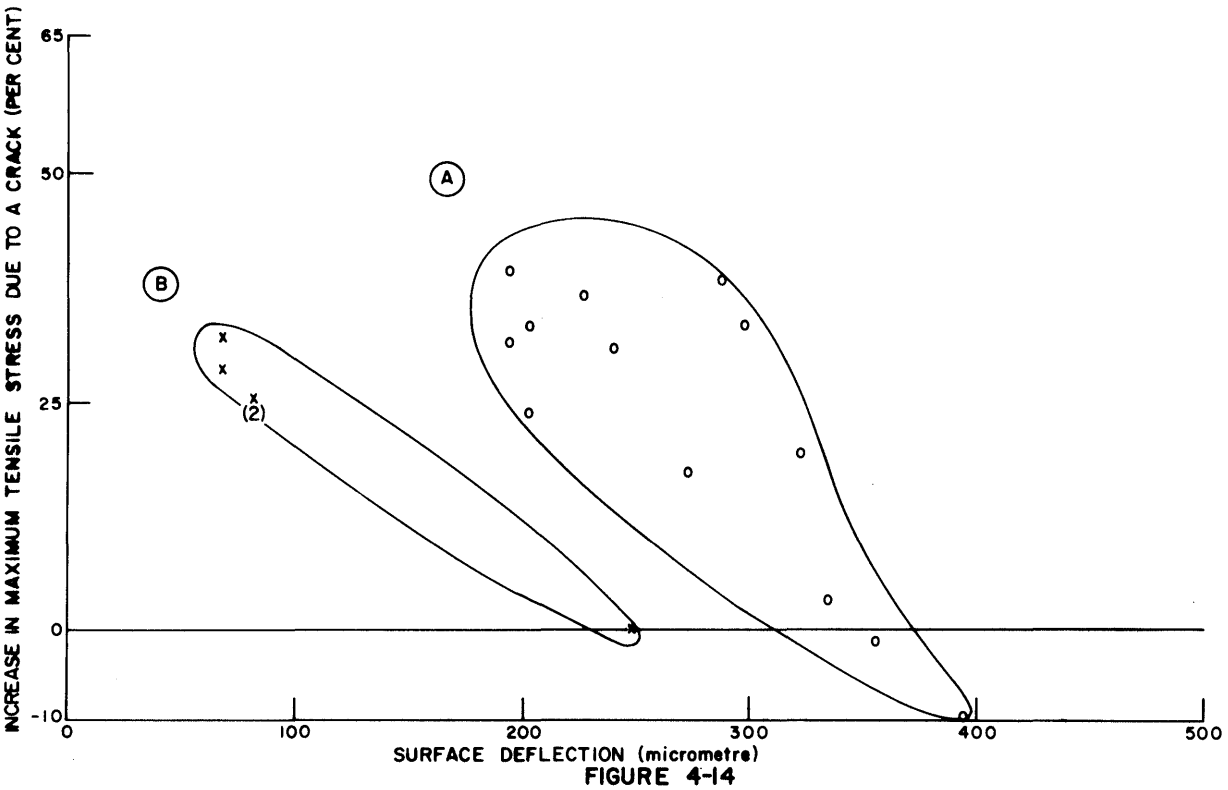

FIGURE 4-14

RELATIONSHIP BETWEEN SURFACE DEFLECTION AND PERCENTAGE INCREASE IN TENSILE STRESS

TABLE 4.4 : Increase in vertical stress and strain in cracked and uncracked pavements

LAY-OUT	FIRST LAYER UNDERLYING CEMENT-TREATED LAYER					SECOND LAYER UNDERLYING CEMENT-TREATED LAYER				
	Vertical stress (kPa)		Vertical strain (με)			Vertical stress (kPa)		Vertical strain (με)		
	Finite elements	CHEVRON	Finite elements	CHEVRON	Ratio	Finite elements	CHEVRON	Finite elements	CHEVRON	Ratio
A	500	161	1 028	331	3,1	110	60	634	346	1,8
	467	111	951	226	4,2	99	47	565	268	2,1
	439	88	888	178	5,0	91	40	516	227	2,3
B	238	34	588	84	7,0	70	16	403	92	4,4
	190	19	450	45	10,0	55	10	303	55	5,5
	162	13	399	32	12,5	46	8	242	42	5,8
C	265	31	675	79	8,5	96	19	520	103	5,0
	231	19	559	46	12,2	80	12	440	66	6,7
	207	14	503	34	14,8	70	10	357	51	7,0
D	189	25	461	61	7,6	58	14	298	72	4,1
	179	19	452	48	9,4	53	12	261	59	4,2
E	344	81	845	199	4,2	39	19	417	203	2,1
F	113	11	277	27	10,3	35	7	165	33	5,0
	134	16	343	41	8,4	42	9	219	47	4,7
G	208	40	1 045	201	5,2	50	21	493	207	2,4
	194	32	897	148	6,1	45	18	433	173	2,5
	191	34	961	171	5,6	46	18	473	185	2,6
	177	28	815	129	6,3	42	16	410	156	2,6

probably take place. The strains in layout H are well below 300 με which is probably due to the intact treated subbase. The low strains in this layout (H) result in a negligible chance of rutting and because of this they were not reproduced in Table 4.4.

4.4 DISCUSSION

4.4.1 Horizontal tensile strain

In the development of a design procedure for a pavement containing a treated layer the presence of cracks has always caused some concern because it has been difficult to evaluate their effect. Tables 4.2 and 4.3 and Figure 4.14 quantify the increase in horizontal tensile stress due to the crack. The increased stress acts parallel to the crack and occurs at the bottom of the treated layer. The increase seems to be dependent on the material properties and structural layout, but it will probably not exceed

about 40 per cent. During the design process it is therefore possible to make provision for the increased stress and to design for it. This can be done by calculating the maximum horizontal tensile stress (σ_t) for the uncracked structural layout, using say CHEVRON. This stress (σ_t) is then increased, for example, 1,4 times and the new value (σ_n) is taken as the design horizontal tensile stress for the material.

4.4.2 Vertical compressive strain

Wide cracks and the corresponding loss of load-transfer result in significant increases in the vertical compressive strains in the lower layers, and the increased strains approach the presently accepted design criterion for relatively dry materials, that is materials at their natural moisture contents. If water penetrates the cracks and becomes trapped in the lower layers it is therefore highly probable that deformation will take place. To avoid this, the penetration of water should be prevented by providing adequate drainage and/or by sealing the cracks effectively. It may also be possible to allow for the strain increase during the design stage and the data in Table 4.4 may be utilized.

The author is not aware of any deformation problems in pavements containing treated layers that can be directly ascribed to the increased vertical stress or strain next to the crack (Wright, 1969; Lewis and Broad, 1969; and Otte, 1973a). This may be because of various reasons such as some amount of load-transfer across the crack which means that the increased vertical strain is not as severe as indicated in Table 4.4; sufficient drainage to prevent wetting of the lower layers; very little attention being paid to this mode of distress even in a severely distressed pavement because it is not really considered as contributory or because it is extremely difficult to isolate and define the various modes of distress.

4.4.3 Crack length, depth and width

In this chapter the length of the crack was considered to be the width of the pavement, that is a transverse crack across the pavement; the depth of the crack was varied, depending on the layout, but it was always taken through the cement-treated layers; and a wide crack was considered (6 mm) across which no load-transfer was assumed to take place. In practice things are different.

The length of the cracks vary and there are shorter cracks which do not extend across the pavement. Shorter cracks were, however, not considered in this chapter because the prismatic solid finite element program

used to perform the analysis can only handle infinitely long cracks extending all the way along the YZ-plane, see Figure 4.1. The increase in stress calculated next to a short crack would probably be less than the increase calculated next to a crack extending all the way across the pavement. This implies that recommendations for stress or strain increases based on the analyses performed in this chapter, are conservative.

Cement-treated materials are brittle, and once a crack has formed it grows very rapidly. This implies that a crack which does not extend through the depth of the layer is not in a stable condition and that it will grow relatively quickly to become a full-depth crack and be in a stable condition. That is why only full-depth cracks were considered in this chapter.

In the analyses only very wide cracks were considered and no load-transfer was assumed to take place across them. In practice there are materials in which the cracks are relatively narrow, from hairline to 2 mm, and some degree of load-transfer will very probably occur across them. In materials known to exhibit narrow cracks, for example some cement-treated natural gravels and lime-treated soils, it is suggested that about 50 per cent load-transfer be assumed and that the stress increases be taken as 50 per cent of those calculated for wide cracks.

4.4.4 Increases recommended for design

If a pavement has to be designed and it is not considered feasible to perform the finite element analysis described in this chapter, the available information can be utilized. Since the increases seem to be dependent on the structural layout and the material properties - which also provide an indication of the crack width - Paterson (1976) interpreted the information in Tables 4.2, 4.3 and 4.4 and proposed Table 4.5. This table indicates the required increases in the results of an uncracked analysis (that is by CHEVRON) and its use is recommended to accommodate the initial crack during structural pavement design work.

Section A.3.3 in Appendix A suggests that these increases are equally applicable to calculated stresses and strains.

TABLE 4.5 : Suggested increases in calculated maximum stresses and strains to accommodate initial cracking

TYPE OF CRACKING	TOTAL THICKNESS TREATED MATERIAL (mm)	MAXIMUM HORIZONTAL TENSILE STRESS*	MAXIMUM VERTICAL STRESS	
			First underlying layer	Second underlying layer
No cracking expected (for example less than 2 per cent lime or cement)		1,0	1,0	1,0
Moderate cracking; crack widths less than 2 mm (for example natural materials with lime or 2-3 per cent cement)	⩽200	1,10	2,5	1,5
	>200	1,20	7,0	3,5
Extensive cracking; crack widths more than 2 mm (for example crushed stone with 4-6 per cent cement)	⩽200	1,25	5,0	2,5
	>200	1,40	14,0	7,0

*Parallel and adjacent to initial crack.

4.5 CONCLUSIONS AND RECOMMENDATIONS

(a) When the prismatic solids finite element program was used to analyse a carefully and properly constructed mesh for an uncracked pavement (Figure 4.4), the differences between the calculated stresses and those obtained from a CHEVRON analysis were generally less than 10 per cent. It is therefore recommended that the prismatic solids finite element program may be used to analyse a pavement containing a cracked treated layer. The finite element mesh should be modelled along the principles that were used to prepare Figure 4.4, and examples of these are Figures 4.5, 4.6 and 4.12.

(b) There are various ways to model a pavement containing a cracked treated layer but the L model is suggested because of the possibility of a loss of vertical bond, and hence continuity, between the treated layer and subbase. The axisymmetric plus asymmetric loading conditions may be used but are not recommended because of the amount of manual labour involved.

(c) After cracking the maximum tensile stress acted parallel to the crack (σ_{zz}) and it occurred near the centre of the loaded area at the bottom of the treated layer.

(d) To calculate the stress increase as a result of the crack it is suggested that the L-model should be used to locate the finite element with the maximum σ_{zz} value. From the stress in the finite element above the one having the maximum σ_{zz}, the stress gradient and the maximum value for the structure can be determined (σ_{mc}). Hereafter the CHEVRON analysis is performed to obtain the maximum value for an uncracked pavement (σ_{mu}). The stress increase as a result of the crack is determined as the difference between the two maximum values, $\sigma_{mc}-\sigma_{mu}$.

(e) A very wide crack with no load transfer across it causes a definite increase in the maximum horizontal tensile stress at the bottom of the treated layer. The increase seems to be dependent on the materials and structural layout. If very wide cracks are expected in the cement-treated material the tensile stress calculated for the uncracked condition should be increased 1,25 times (if the expected total thickness of the treated layers is less than or equal to 200 mm), and by 1,4 times if the expected total thickness is more than 200 mm. If moderate cracking is expected, the corresponding increases should be only 1,1 and 1,2 times respectively. It is suggested that these increases be accepted and that the treated layer be designed accordingly.

(f) The increase in the vertical stress and strain in the subgrade as a result of the initial crack is significant and the possibility of subgrade deformation may not be excluded. It is suggested that more attention should be paid to it, for example by providing adequate drainage. The increases reported in Table 4.5 should be used for pavement design work.

(g) This computer analysis contributed to a better understanding of the stress distribution and possible behaviour of a pavement containing a cracked treated layer. Further expansion and work along these lines may eventually result in a complete understanding thereof.

CHAPTER 5

THERMAL STRESSES AND INSULATION

5.1 INTRODUCTION

When the first pavement design theories were developed, those during the thirties and forties, traffic-associated distress was the major consideration. An example is the California Bearing Ratio (CBR) procedure that was developed to overcome traffic-associated deformation of the subgrade and which was based on only wheel load intensity. Later, when a regional pavement design procedure (for example the method from the AASHO Road Test) was to be extended to a wider geographical area, it was realised that environmental factors do play an important part. Non-traffic-associated (that is environmental) distress is therefore presently considered equally as important as traffic-associated distress. The growing interest in the effect of the environment, currently sub-divided into moisture and thermal effects, can be seen in the proceedings of the three International Conferences on the Structural Design of Asphalt Pavements - the first and second contained no reports on these subjects, while the third (1972) had four.

This chapter deals with only one aspect of environment, namely the effect of temperature on a pavement containing a treated layer. In this chapter the term 'treated' is used to mean either cement- or lime-treatment (Otte, 1976). There are a number of ways of calculating the temperature distribution but the finite difference technique developed by Williamson (1972a) was used. He developed a mathematical model and prepared a computer program as the first phase of a research project on the effects of environmental factors. This chapter presents some of the results of the second phase which is the civil engineering application of the model. The objectives are to study qualitatively (i) the diurnal variation in stress in the treated layers, (ii) the insulating ability of various thicknesses and types of material, and (iii) the effect of a crack on the thermal stresses.

5.2 BACKGROUND

The importance of thermal gradients on concrete, that is rigid, slabs has been known since the twenties (Westergaard, 1927). One of the first studies (Lister, 1972) on the importance of thermal stresses in pavements containing treated layers mentioned that "...the stresses developed on cooling, together with those due to shrinkage on setting and hardening of the cement after construction, are responsible for the characteristic regular pattern of transverse cracking observed in cement-bound bases...";

and that the thermal stresses are "...comparable to the magnitude of traffic induced stresses...". Williamson (1972a) described a practical case which tended to confirm that the initial cracking in a cement-treated layer is due to temperature gradients in the material.

It is therefore very important to try to minimize the temperature gradient. Possible ways are by the use of insulating materials, heating or cooling elements, or the control of energy influx into the pavement (Williamson, 1972b). Williamson claimed that the use of heating or cooling elements in pavements would be impractical and very expensive, and he described some ways of reducing the energy influx, for example by having a light-coloured surface. The insulation method seems practical but it depends on the physical properties of the material, for example specific heat, density and thermal conductivity. These properties are in turn affected by others, such as the degree of compaction, moisture content and geological origin. This makes the number of variables virtually unlimited. He discussed the use of bituminous layers to insulate the treated layer against severe temperature gradients. The author believes that the untreated crusher-run base, which is very often used on top of the treated layer (Otte and Monismith, 1976) is also suitable as an insulation layer. Since crusher-run materials are cheaper than bituminous materials, it is worthwhile to investigate their insulating properties with the possibility of using them in preference to bituminous materials.

5.3 ANALYSIS

5.3.1 Structural layout

The basic structural layout considered in the analyses is shown in Figure 5.1; it consists of a surface treatment, a 150 mm untreated crusher-run base, two 125 mm cement-treated natural gravel layers, and a 125 mm untreated subbase. During the analyses the thickness of the crusher-run base was increased to 300 and 450 mm and it was also removed completely. The analyses were also repeated using a bituminous base instead of the crusher-run. The Poisson ratios of the materials were fixed at 0,35 and the elastic moduli are given in Table 5.1.

5.3.2 Computer program

A slightly modified version of the Macro Environmental Simulation Model (MESM) of Williamson (1972) was used. The major modification was the way in which the initial temperature distribution was specified and calculated (Otte, 1976a).

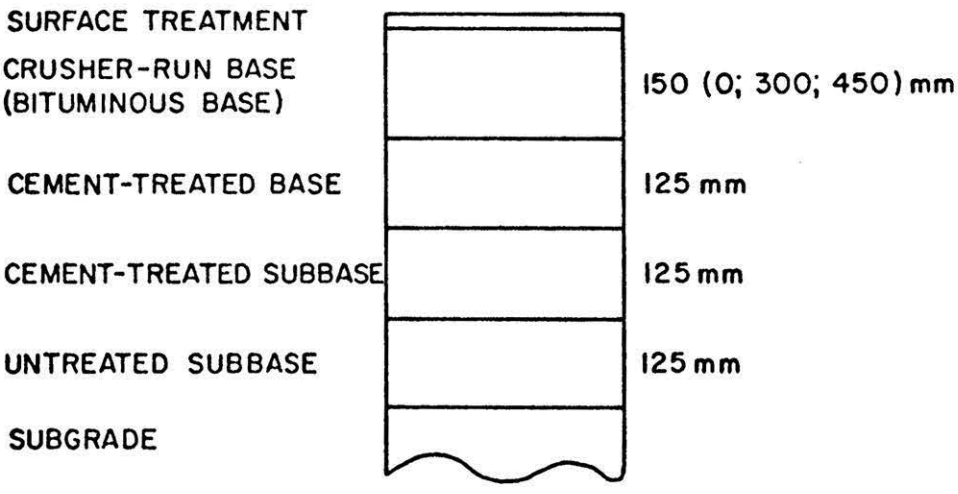

THE VARIATIONS WHICH WERE CONSIDERED DURING THE ANALYSIS ARE SHOWN IN BRACKETS

FIGURE 5-1

THE BASIC STRUCTURAL LAYOUT FOR THE THERMAL ANALYSIS

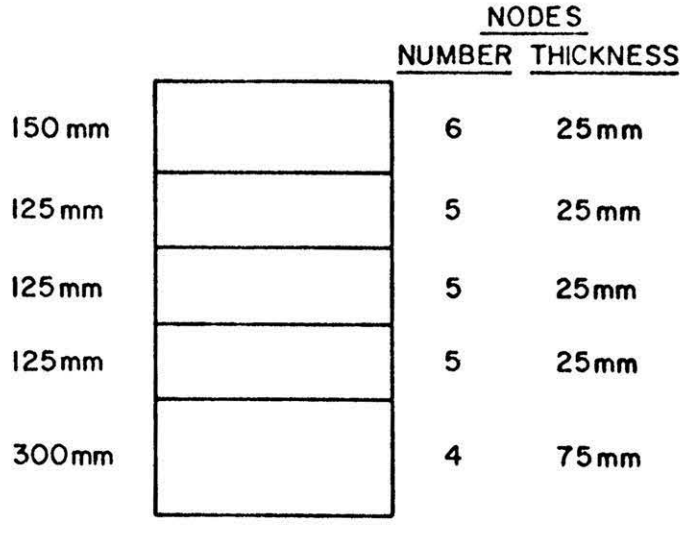

FIGURE 5-2

SUBLAYERING INTO NODES

TABLE 5.1 : Elastic moduli of materials used in the thermal analysis

MATERIAL	ELASTIC MODULUS (MPa)
Crusher-run	500
Cement-treated natural gravel base	8 000
Cement-treated natural gravel subbase	4 000
Untreated subbase	300
Subgrade	100
Bituminous material	3 000

The modified program required the pavement to be divided into sublayers (nodes) and 25 were chosen: 6 for the upper layer, 5 for each of the following three layers, and 4 for the subgrade (Figure 5.2). The thickness of the upper layers and the number of nodes were such that the sublayers were 25 mm thick. The thermal effect of the subgrade, that is the depth which affects the calculated temperatures, was considered to be 300 mm and it was divided into four 75 mm sublayers. When the thickness of the upper layer was increased, the number of sublayers remained 6, resulting in the sublayer thickness increasing to 50 and 75 mm. Some analytical work during which the thick upper layers were subdivided into more than six 25 mm sublayers, indicated a significant difference from that obtained when six relatively thick sublayers were used, that is when the number rather than the thickness of the layers was increased. The variation in results may be a computation problem and it was decided to accept six thicker sublayers rather than numerous 25 mm sublayers. This may have had an effect on the actual thermal stress values which are reported later.

The analyses were performed with the data set stored in the computer program for the average mean climatical data of Pretoria, South Africa. The temperature calculation was started with a uniform temperature distribution of 20 ^{o}C, but during the analysis it was adjusted very rapidly and hence complied with the temperature gradient for Pretoria.

5.3.3 Material properties

Two types of crusher-run were considered; according to their thermal conductivities, the one was a granite and the other a quartzite (Bullard, 1939). They were each considered at two densities - at 88 and 82 per cent of the solid density of the particles and were called dense and loose (see

Appendix C). In the study the quartzite was considered as the basic material and the granite was compared with it. The thermal conductivity and specific heat of the materials in the other layers were obtained from the catalogue of average mean values contained in the computer program, because the number of variables had to be kept to a minimum. Table 5.2 contains a summary of the thermal properties used during the analyses.

TABLE 5.2 : Thermal properties used during the analyses

PROPERTY	BITUMINOUS MATERIAL	CRUSHER-RUN				TREATED BASE AND SUBBASE	UNTREATED SUBBASE	SUBGRADE
		Granite		Quartzite				
		Loose	Dense	Loose	Dense			
Conductivity (cal/cm.s.^{o}C)	0,007	0,0032	0,0042	0,0067	0,0093	0,005	0,003	0,002
Specific heat (cal/g^{o}C)	0,20	0,20	0,20	0,20	0,20	0,20	0,20	0,18
Density (g/cc)	2,2	2,14	2,31	2,2	2,36	2,1	1,9	1,8

The absorptance and emittance were fixed at 0,95 which implies a dark surface such as a prime or a thin surface treatment on the crusher-run. Williamson (1972a) evaluated the importance of these coefficients and since the absorption coefficient has a significant influence on the surface temperature it was decided to keep these values constant throughout the analyses.

The coefficient of thermal expansion of the two cement-treated layers was fixed at $4{,}5.10^{-6}$ per ^{o}C. Based on previous laboratory studies (Otte, 1974) and assuming the tensile strength to be half the flexural strength, the tensile strengths of the upper and lower cement-treated natural gravels were fixed at 350 and 120 kPa, respectively. The coefficient of subgrade restraint was fixed at 0,90.

5.4 DIURNAL AND ANNUAL VARIATIONS

The results from the computer analyses can be presented in many ways and it is possible to prepare several graphs showing the diurnal and annual variations in stress through the treated materials. Since this is a design-orientated study, only the stresses at the bottom of the treated layer are considered because it is expected that when the traffic-associated stresses are included, this position will experience the maximum total stress.

5.4.1 Diurnal variation

Figure 5.3 shows that the magnitude of the thermal stress in the upper treated layer varies considerably throughout an average day in December. Unlike the traffic-associated stresses, the maximum thermal stress seldom occurs at the bottom of the treated layer. The variation in stress with depth is small in comparison with the diurnal variation.

Figure 5.4 shows a typical variation in stress at the bottom of each of the two treated layers. These locations experienced tensile stresses in the morning, around midday they were stress-free, and in the afternoon they went into compression. The time of the highest tensile stress, which is the critical time with regard to cracking, is during the morning with a peak around 7 to 8 o'clock. This same pattern also applied to each of the other months of the year. The critical time for cracking differs significantly from what Lister (1972) calculated, since he found it to be the early afternoon.

Figures 5.5 and 5.6 show typical variations in the number of equivalent 80 kN axles during typical days on six South African roads (note the difference in vertical scale). Since the heavy axles contribute significantly to the number of equivalent axles, these distributions may be taken as an indication of the hourly distribution of heavy axles. This information was obtained with the Axle Weight Analyser (AWA) (Basson et al, 1972) and consisted of hourly counts during day-time but only an average from dusk till dawn. It shows that the load distribution varies from road to road with very little of a standard distribution although the low night-time averages indicate that the bulk of the heavier traffic travels during the day when both the tensile and compressive thermal stress peaks occur. Since the tensile stress peak contributes to failure and the compressive peak cannot 'heal' the damage done during the tensile peak, they do not really cancel out and the effect of the tensile peaks is cumulative. It would therefore be beneficial if the traffic loading, and hence the traffic-associated tensile stresses, could be minimized during the periods of peak thermal tensile stresses and maximized during periods of peak thermal compressive stresses, for example between 13h00 and 16h00. Since the traffic seems to be slightly lighter during night-time, it would also be beneficial if the structural layout and material properties could be changed in such a way that the peak tensile stress would occur during the night and not during the day.

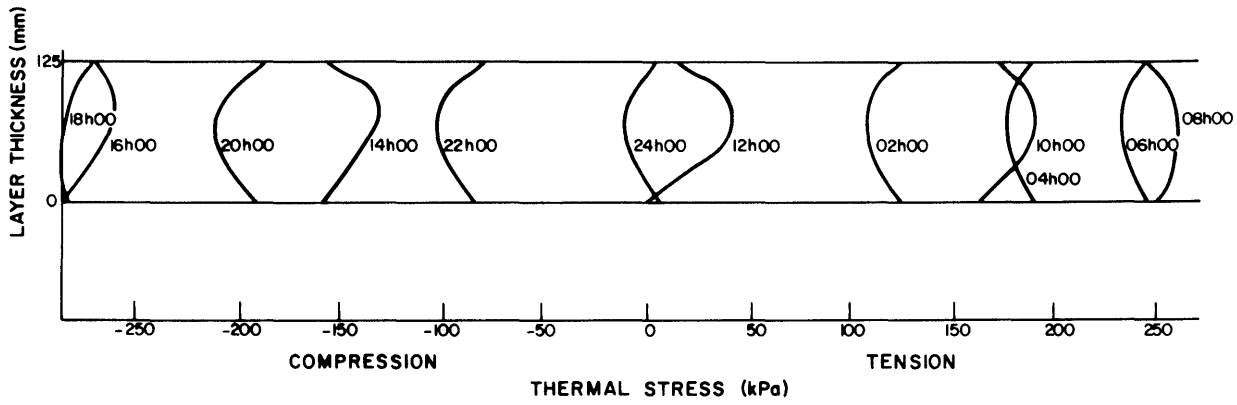

FIGURE 5-3

DIURNAL STRESS DISTRIBUTION WITH DEPTH IN THE UPPER UNCRACKED TREATED LAYER

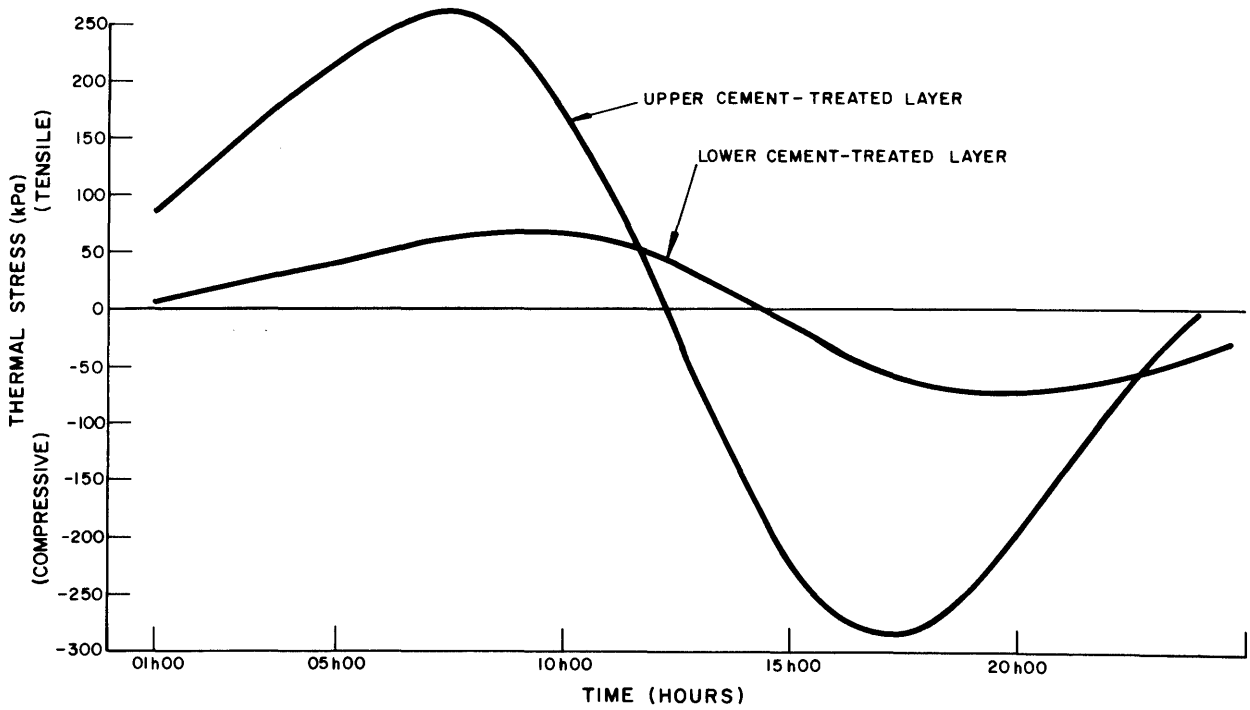

FIGURE 5-4

TYPICAL DIURNAL VARIATION IN THERMAL STRESS DURING DECEMBER IN TWO UNCRACKED CEMENT-TREATED LAYERS UNDER 150mm CRUSHER-RUN

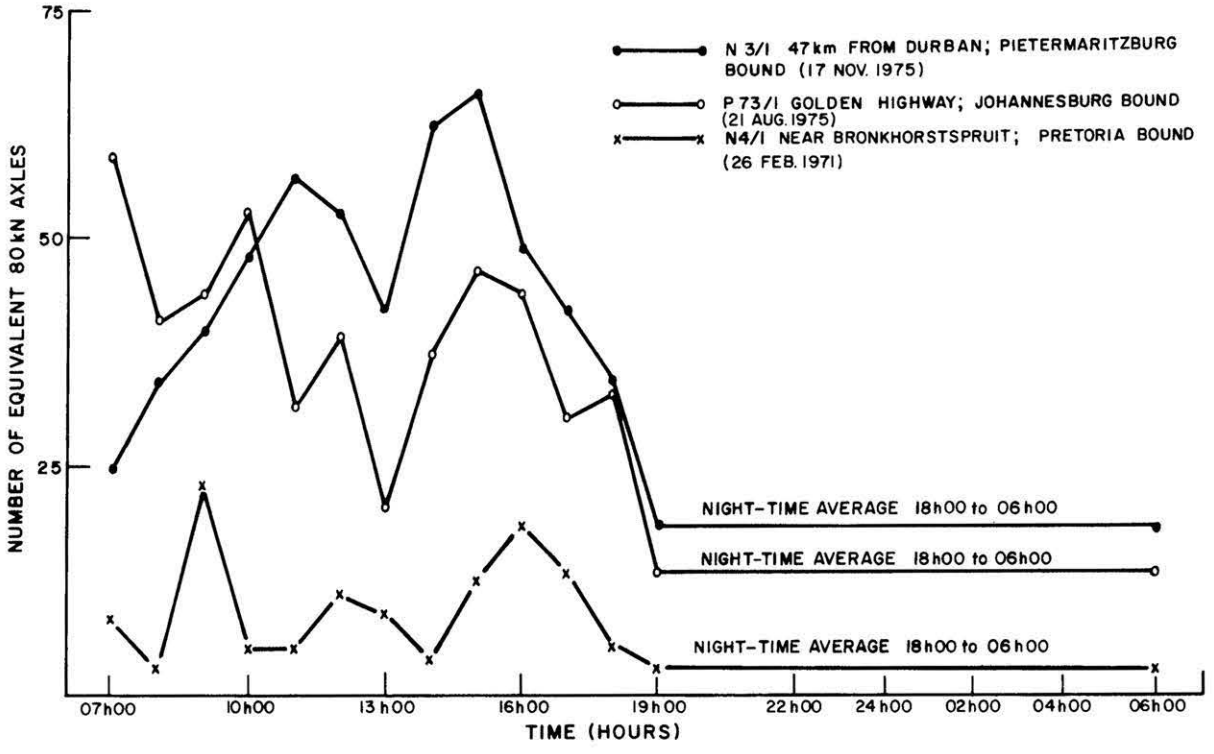

FIGURE 5-5
DIURNAL VARIATION IN EQUIVALENT TRAFFIC ON THREE ROADS

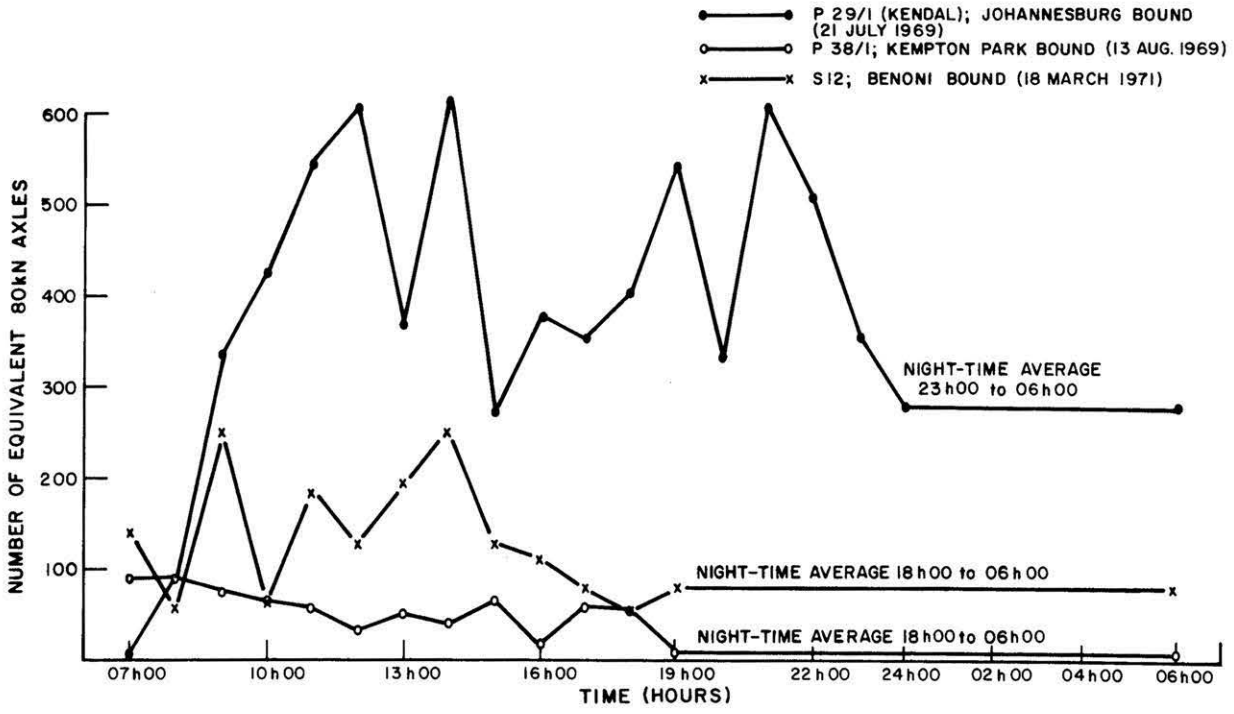

FIGURE 5-6
DIURNAL VARIATION IN EQUIVALENT TRAFFIC ON THREE ROADS

5.4.2 Annual variations

Figure 5.7 shows the theoretical annual variation in the daily maximum tensile and compressive stress at the bottom of the two treated layers of the basic structural layout when it is located in Pretoria. Average material properties were used for the crusher-run in this layout (Williamson, 1972) and the thermal conductivity and density were taken as 0,006 cal/cm.s.^{o}C and 2,2 g/cc respectively. The figure shows that both the maximum tensile and compressive stresses occur during December and the minima during June. This same tendency was observed for all the designs analysed in this study and, unless otherwise stated, the tensile stress values reported in this chapter are the maxima which occurred during December.

5.4.3 Combined traffic-associated and thermal stresses

The traffic-associated tensile stresses under a 40 kN wheel load (520 kPa tyre contact pressure) were calculated, using the CHEVRON computer program, as -509 and 209 kPa for the top and bottom of the upper treated layer, and as 67 and 331 kPa for the top and bottom of the lower treated layer. These stresses were added to the thermal stresses and presented as Figure 5.8. It shows that although the thermal stresses are highest in the upper layer, the total stresses (traffic-associated plus thermal) are highest in the lower layer. The bottom of the lower layer is thus the critical position in practice.

5.4.4 Discussion

It appears that the maximum thermal stresses in the two cement-treated layers developed during the mornings of December. It should be stressed that these are only average values and the occurrence of the true maxima are dependent on numerous environmental and climatic factors.

The thermal stresses in the lower cement-treated layer were very much less than those in the upper layer. Once the traffic-associated stress had been added, the stress position was reversed and the maximum total tensile stress occurred at the bottom of the lower layer.

5.5 THERMAL INSULATION

The use of insulating materials to attenuate temperature gradients is practical and it is considered advisable that they should be used to insulate treated layers in pavements. The insulating ability of the various materials should however be studied before practical recommendations can be made on how they should be used.

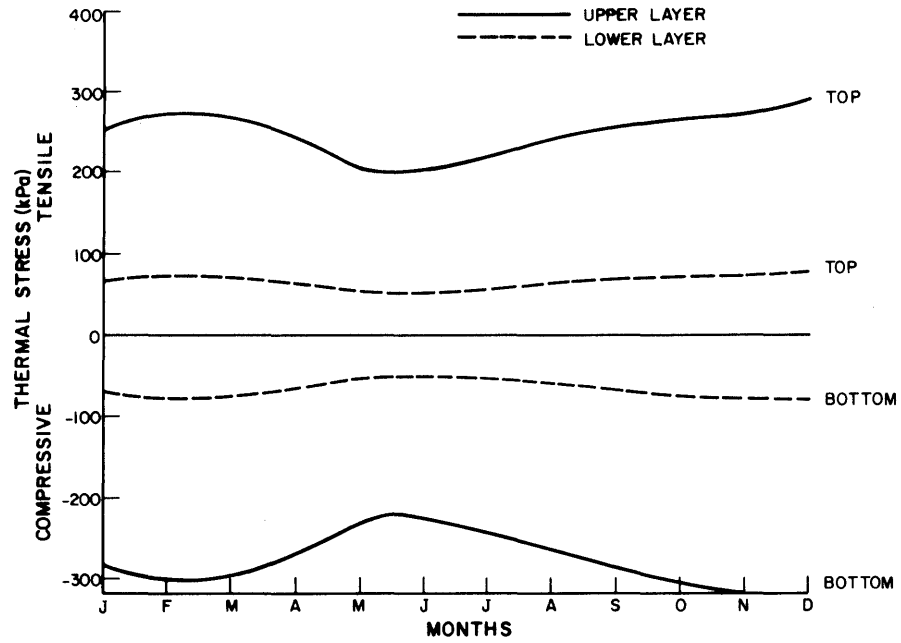

FIGURE 5-7

ANNUAL VARIATION IN DAILY MAXIMUM THERMAL STRESS AT TOP AND BOTTOM OF UNCRACKED LAYERS.

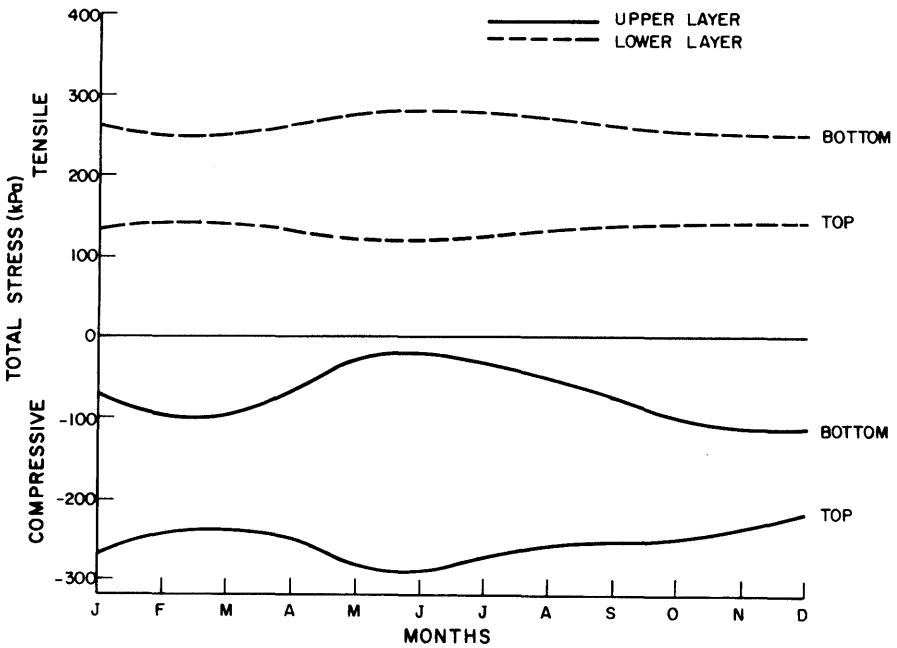

FIGURE 5-8

ANNUAL VARIATION IN DAILY MAXIMUM TOTAL STRESS AT TOP AND BOTTOM OF UNCRACKED LAYERS.

Heat transfer in road pavements may be described as an unsteady state problem since the heat input, for example the solar radiation, does not remain constant throughout the day but it varies from time to time. This problem is therefore also covered by the unsteady-state one-dimensional heat conduction formula (Hsu, 1963)

$$\frac{\delta T}{\delta t} = D\frac{\delta^2 T}{\delta x^2} \quad \text{.......................................} \quad (5.1)$$

where T = temperature

t = time

x = distance

D = diffusivity

The amount of heat transfer is governed by the thermal diffusivity which is defined as

$$D = \frac{k}{s\rho} \quad \text{..} \quad (5.2)$$

where k = thermal conductivity

s = specific heat

ρ = density

The diffusivity is a combination of the material's ability to conduct the heat through it (conductivity) and to store or retain it (density times specific heat).

In a pavement with an insulating layer the amount of heat transfer through this layer and into the treated layers is the matter for concern. The thermal diffusivity of the insulating layer should be low since this will result in the least heat transfer and hence the maximum insulation, and this in turn will cause smaller thermal gradients in the lower layers. A reduction in the diffusivity can be achieved by (i) reducing the conductivity so that the material cannot conduct the heat through it, or (ii) by increasing the density and specific heat which will enable the material to retain more heat in itself. One should therefore theoretically be able to reduce the diffusivity, and hence increase the insulating ability, of say a soil or crusher-run, by increasing its density. The opposite, however, usually happens after an increase in density. The diffusivity actually increases because the increase in conductivity, as a result of the removal of air from between the grains, exceeds the increase in density (see Appendix C).

5.5.1 Material type and quality

Figure 5.9 shows the effect of changes in the diffusivity of the insulating material on the maximum thermal tensile stresses in the basic layout (Figure 5.1). The changes in diffusivity were brought about by considering two types of crusher-run (quartzitic and granitic) at two densities, and one bituminous material. The figure shows that the thermal tensile stresses at the bottom of the two layers decreases only slightly with an increase in diffusivity. This figure may be used to evaluate the effect of further changes in the density and rock-type of the crusher-run insulating layer. It seems, however, that the insulation is relatively independent of these parameters and that a change in rock-type and density will produce only second order changes in the thermal stress values.

5.5.2 Thickness of insulator

Figure 5.10 shows the reduction in thermal stress with an increase in the thickness of the insulator. When this figure is compared with Figure 5.9 it becomes clear that the thickness of the insulator is much more important than the type and quality of the material because there is very little difference between using a bituminous material and a crusher-run as the insulator. In all instances the insulation succeeded in preventing thermal cracking of the treated layers because the thermal stresses were below the tensile strengths specified in section 5.3.3. An analysis in which the insulation was removed showed that thermal cracking would occur very quickly in both of the two treated layers - even before sunrise. The program predicted the crack spacing at about 11 metres; this result differs from the author's practical observations of generally 3 to 6 m. The relatively large spacings may be a result of the relatively high tensile strengths that were specified, 350 and 120 kPa.

An interesting observation is the shape of the curves for the two materials in Figure 5.10 - convex for quartzite and concave for granite. One should however not rely very quantitatively on these curves and the stress values shown in the figure because, as was explained in section 5.3.2, the thickness and number of sublayers used for the insulator has an effect and this does influence the values and the shape of the curves.

5.5.3 Cracked treated layers

It was mentioned above that both of the two treated layers will crack if no insulator is used. Figure 5.10 and all the previous figures were prepared for intact treated layers and are therefore of very little practical

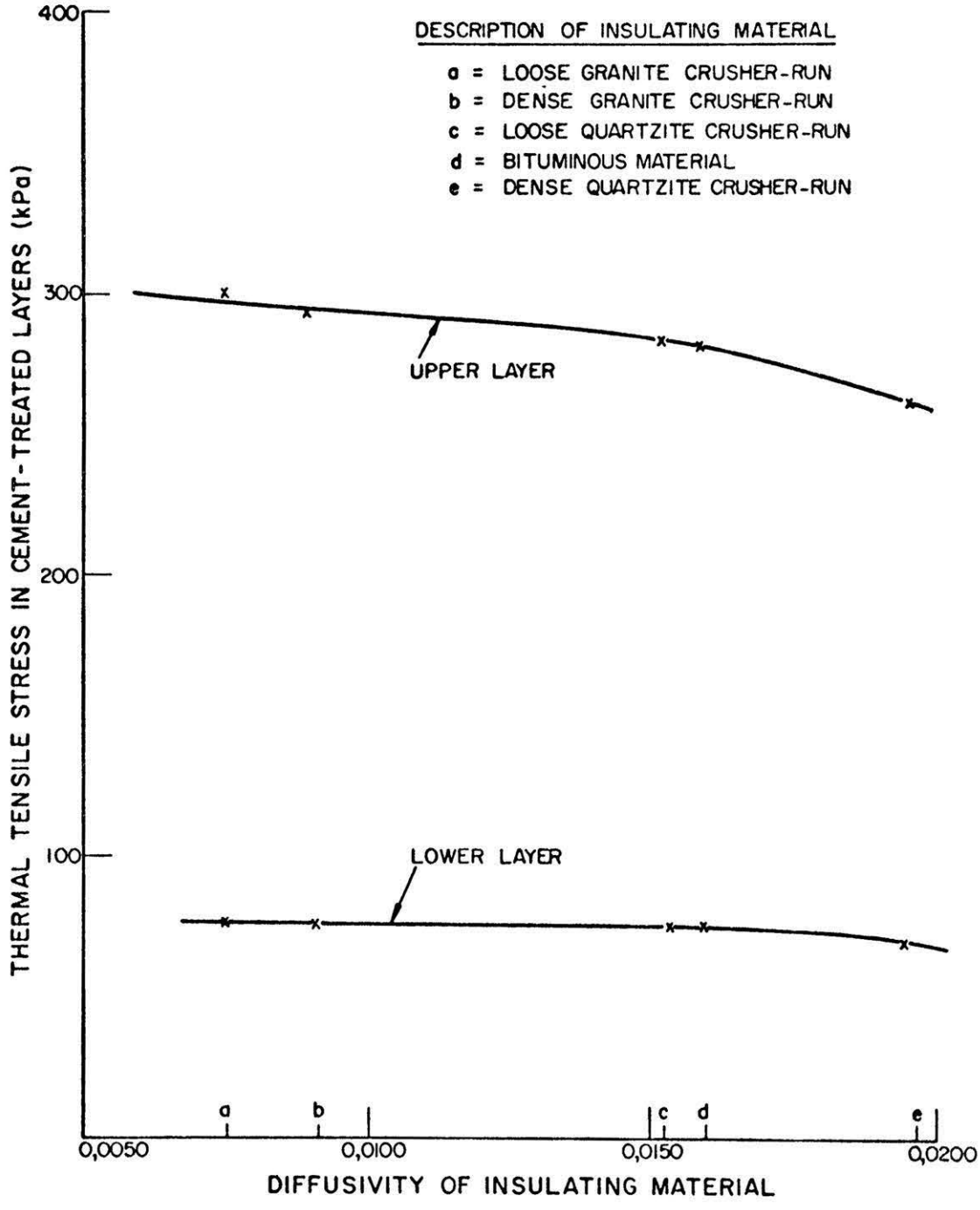

FIGURE 5-9

EFFECT OF DIFFUSIVITY ON MAXIMUM THERMAL TENSILE STRESS

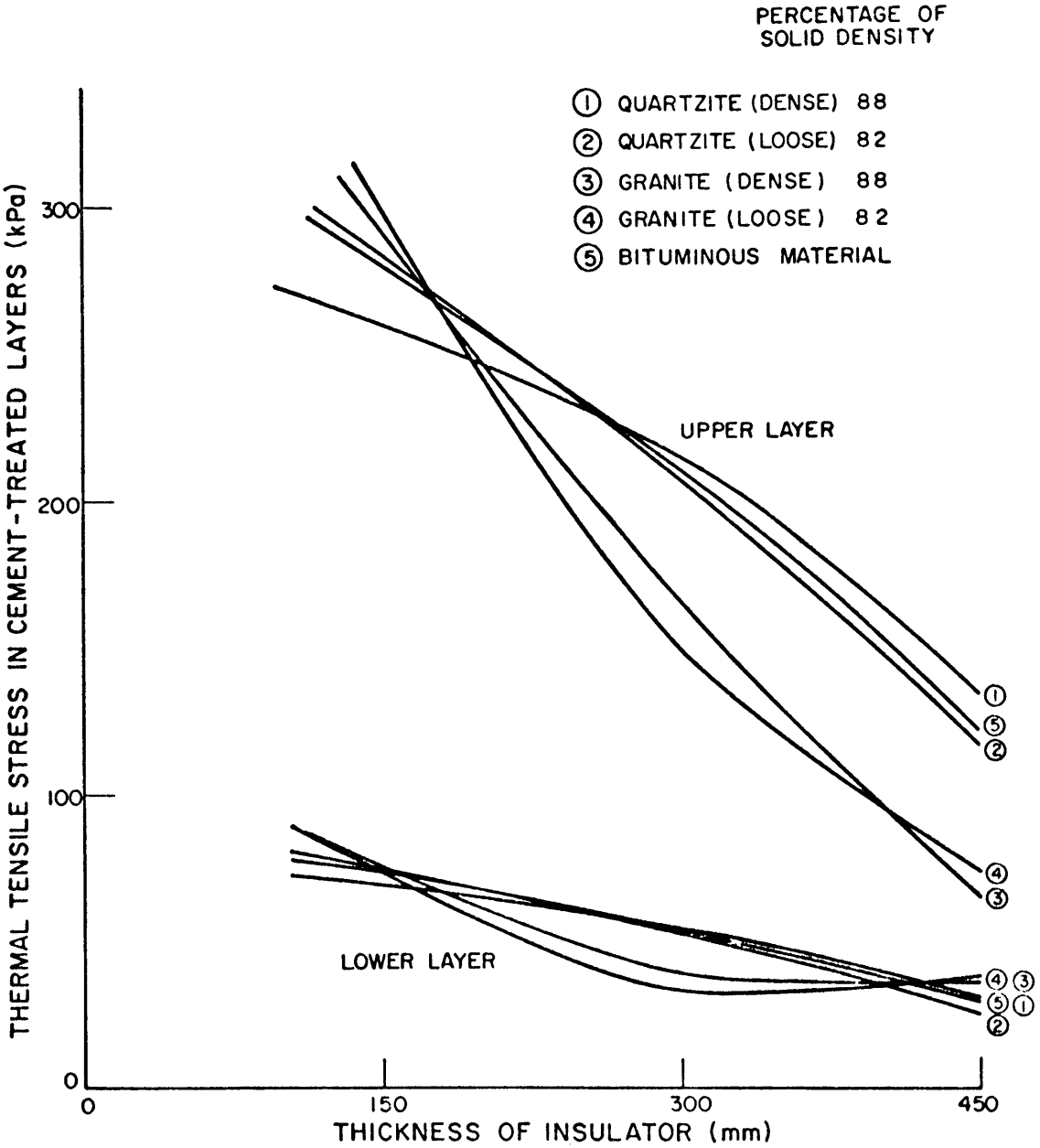

FIGURE 5-10

EFFECT OF INSULATING LAYER ON THERMAL TENSILE STRESS

significance since there often is quite a delay between the construction of the treated layer and the completion of the crusher-run insulator. During this period the treated material hardens and, depending on the hardening rate, the temperature cycles and the material quality, it will crack. If temperature is not the cause of the cracking, then shrinkage will be, but cracking is virtually inevitable. To obtain a fairly practical result on insulation, the analyses had to be repeated and cracked treated layers were assumed. Based on the results of the analyses with no insulating layer, the crack spacing and width were taken as 11 metres and 0,3 mm respectively.

The analyses of cracked treated layers showed a marked reduction in maximum thermal tensile stresses. This is quite probably due to the presence of the crack which allows some movement to take place and hence relieves the build-up in stress. The analysis with no insulating layer indicated the maximum thermal tensile stresses at the bottom of the two cracked treated layers to be very high; 150 mm dense quartzitic crusher-run was capable of reducing these values to less than about 140 and 2 kPa respectively, while 450 mm crusher-run reduced both to below 4 kPa.

The crack spacing in cement-treated natural gravel bases in South Africa varies from road to road and it is very difficult to define an average spacing. It was, however, felt that the 11 m used in the previous analyses was too long because the tensile strengths used to calculate it corresponded to those attained only after the material had been in place for some time. The material is more likely to crack at an earlier age while the tensile strength is still low, and this will result in closer crack spacings. Based on the author's observations 6 m was chosen as the average. Assuming the crack width as 0,3 mm, a 150 mm crusher-run insulator succeeded in keeping the maximum tensile stresses below 11 and 5 kPa respectively. When the crack width was significantly reduced, to only 0,1 mm, the maximum tensile stresses increased to about 175 and 45 kPa respectively. The calculated thermal movements at the crack openings were very small, only about 0,1 to 0,3 mm, and this may explain why 150 mm crusher-run is usually adequate to prevent completely the cracks in cement-treated natural materials from appearing on the road surface.

Figure 5.10 indicates that an insulator of about 450 mm is necessary to reduce the thermal stresses in uncracked treated layers to less than about 140 kPa. From the previous discussion it appears that this can also be achieved by only 150 mm crusher-run, provided the layer is slightly cracked and movement may take place. Since it is virtually impossible to

avoid cracking in a properly constructed cement-treated layer it will always have this form of stress relief. It is therefore suggested that 150 mm crusher-run is adequate and should be provided as a thermal insulator on cement-treated materials because (i) this is a practical thickness from a construction point of view, (ii) it will prevent the cracks in the treated layers from propagating to the surface, and (iii) it is usually cheaper than a comparable thickness of bituminous material.

5.6 THERMAL STRESSES IN OTHER PAVEMENTS

The previous analyses were done for only one design layout. To study the applicability of the observations to other layouts it was decided to analyse the structural layout that was used on Special Road S12 between Cloverdene and Argent, and on National Route N4/1 between Pretoria and Bronkhorstspruit (Otte, 1973a).

The pavements consist of 25 mm asphaltic concrete surfacing, 100 mm cement-treated crusher-run, 100 mm untreated crusher-run, 100 mm cement-treated natural gravel subbase and some selected subgrade. The material properties and other details required to run the computer program are summarized in Appendix D.

Assuming an uncracked cement-treated crusher-run base (elastic modulus = 18 500 MPa) it was calculated that the layer would crack at 19,9 m spacing and the crack openings would be about 1 mm. The associated maximum thermal tensile stress after cracking was about 500 kPa. The large crack spacing was caused by the high tensile strength and, because the cracks would probably have formed while the strength was still low, it was decided to repeat the analysis. During the earlier crack measurements on the pavements (Otte, 1973a), the crack spacing and width were recorded as about 4 m and 1 mm respectively. The analysis was repeated for a pavement cracked accordingly and the maximum thermal tensile stress was less than 10 kPa.

The same general observations therefore apply to both types of structural layout and hence possibly to all layouts with cement-treated layers. The thermal stresses are very high in an uncracked layer, but in a cracked layer, and all properly constructed cement-treated layers do crack initially, movement can take place at the crack openings and this reduces the thermal stresses significantly.

5.7 DISCUSSION

The theoretical analysis indicated that thermal stresses were very detrimental in uncracked treated layers and that their magnitudes were comparable to those of the traffic-associated stresses. They should therefore be reduced and a practical way is to provide an insulating layer, for example crusher-run or bituminous materials, on top of the treated layer. Theory also indicated the thickness of the insulator to be much more important than the type of material used and its thermal properties.

A properly constructed cement-treated layer will crack at a relatively early age and the crack spacing will be much less than that calculated from the material properties after hardening. After initial cracking the chances of further thermal cracking become very slim because the slabs are short (4 to 6 m), movement can take place which eliminates a build-up of thermal stress, and the tensile strength continues to increase. The amount of thermal stressing in these shorter slabs is very small, and in comparison with traffic-associated stresses it may be neglected. The relative unimportance of thermal stresses in cracked treated layers may be one of the reasons why no need has ever arisen for considering them in the existing pavement design procedures.

5.8 CONCLUSIONS

(a) The computer program of the Macro Environmental Simulation Model (MESM) was found to be very suitable for the analysis of temperature distributions and the associated thermal stresses in pavements. It is thought to be the only program capable of computing thermal stresses in a cracked pavement layer.

(b) The position of the maximum thermal tensile stress during the day varies throughout the depth of the pavement. It may however be assumed that in uncracked treated layers the maximum value required for pavement design purposes occurs at the bottom of the treated layers during the mornings in December. In cracked treated layers there are more variations and, depending on the layout, the maximum thermal stress may occur at virtually any hour.

(c) The thickness of the insulator is much more important than the type of material used. The selection of the insulating material is therefore not governed by its thermal properties but by others, for example its load-bearing ability.

(d) The usual construction sequence and the material properties are such that cement-treated layers will crack, either due to temperature or shrinkage, and they should be considered as cracked. The small movements of the fine cracks are sufficient to eliminate a build-up in thermal stresses and the resulting stresses are significantly smaller than those calculated for uncracked layers. The importance and possible influence of thermal stresses on pavement performance is therefore significantly reduced by the fine cracks which are present in the material.

(e) The amount of thermal movement at the cracks is relatively small (0,1 to 0,3 mm) and 150 mm crusher-run is considered adequate to dampen the cracks completely and prevent them from appearing on the pavement's surface.

(f) The use of a 150 mm crusher-run layer on top of the treated layer will also help to insulate the treated layer against thermal stresses.

(g) The outcome of this study was quite unexpected in the light of previous thinking on thermal stresses in treated layers. Previously thermal stresses were considered to be very important but this study has shown it to be true only for uncracked treated layers. Once the cracks have developed the thermal stresses become virtually negligible in comparison with the traffic-associated stresses. Thermal stresses may therefore be considered as unimportant in cracked treated layers.

CHAPTER 6

VARIATIONS IN QUALITY ARISING DURING CONSTRUCTION

6.1 INTRODUCTION

It is important that the properties of the materials produced during construction should correspond to those assumed by the designer when he does the design. This correspondence is generally assumed because it is accepted that the instituted construction controls, for example field density tests and compliance with the construction methods outlined in the specification, are adequate to ensure it. Variations in the specifications of consulting engineers and differences between the construction techniques, that is mixing, compacting and curing, used by the various constructing organizations, both public and private, are considered significant and it is believed that their effect should be evaluated. The effect of all these aspects on the properties of cement-treated materials has been studied extensively - but individually. The author believes that the combined effects and interaction should be studied under the general heading of construction technique.

The objectives of this chapter are therefore (i) to study the variation in the properties of cement-treated materials constructed in the field, and (ii) to compare the properties of field-constructed materials with those of materials prepared in a laboratory under ideal conditions. The outcome can possibly be utilized in the development of a rational pavement design method since it will indicate to the designer what allowance he should make to accommodate the construction process.

6.2 LITERATURE REVIEW

One of the first studies on the difference between field strengths and the design values was performed by Robinson (1952). In his case the difference was largely caused by an insufficient distribution of the cement through a silty clay. He showed that if the mixing efficiency could be increased and a more even distribution of the cement could be obtained, less cement would be required to comply with the specified strength. Since this represented about a 30 per cent reduction in total additive required, it could mean a significant financial saving on large contracts. This serves to show the importance of efficient mixing in reducing the difference in strength between field- and laboratory-prepared samples.

Mitchell and Freitag (1959) reported that British engineers "...found that normal construction methods result in a field strength equal to about 60% of the laboratory strength for a given cement treatment...". The cement content should therefore be determined as the amount necessary to

obtain a laboratory compressive strength equal to the required strength divided by 0,6. This implies that if a strength of 1 700 kPa is required, the laboratory strength should be 2 800 kPa. The recommendation by Ingles and Metcalf (1972) seems to have been based on this work.

Wang (1968) performed compressive and bending tests on both field- and laboratory-prepared cement-treated materials. He compared the strengths and elastic moduli and Table 6.1 summarizes his results. He could not recover beam samples for testing from the materials treated with 6 per cent cement until two months after their construction and no beam samples could be recovered from the 3 per cent cement section because the materials were too weak.

TABLE 6.1 : Comparison in properties of field- and laboratory-prepared specimens (from Wang, 1968)

MATERIAL PROPERTIES			FIELD-PREPARED	LABORATORY-PREPARED	RATIO OF FIELD- TO LABORATORY-PREPARED
Strengths	Unconfined compressive strengths (kPa)	3% cement	140- 340	410- 760	0,33-0,45
		6% cement	415-1 030	760-1 720	0,55-0,60
	Bending strengths (kPa)	3% cement	*	100- 280	*
		6% cement	*- 450	380- 660	*-0,69
Elastic Modulus	Compression (MPa)	3% cement	70- 660	280-1 030	0,25-0,64
		6% cement	140-1 170	1 000-2 200	0,13-0,53
	Bending (MPa)	3% cement	*	410-1 240	*
		6% cement	*-1 720	900-3 030	*-0,57
*Too weak to be sampled and tested.					

Wang (1968) obtained the same densities in the field as in the laboratory; nevertheless both the strength and elastic modulus of the field samples were only about 50 to 60 per cent of the corresponding laboratory samples. He gave the possible reasons for the difference as -

(a) better mixing in the laboratory than in the field;
(b) curing conditions in the field not as effective as in the laboratory;
(c) disturbance of field samples during cutting and extraction.

He stated that "...Among the possible causes, the effect of low efficiency mixing seems to be a major factor. In addition, the differences

in curing condition might be quite significant...". This implies that he was not very sure of the cause of the differences.

Fossberg (1970) recorded the differences between three construction conditions namely (a) mixing in a ready-mix concrete truck (called truck mixing) and field compaction, (b) truck mixing and laboratory compaction, and (c) laboratory mixing and compaction. About the same densities were obtained in all three conditions and the recorded strength and elastic modulus values are shown against curing time in Figure 6.1. The differences were very small and he obtained about the same strength and elastic modulus for all three construction conditions. He did however observe structural anisotropy in the field-compacted materials, that is the elastic modulus in the direction of compaction was about 1,5 times lower than in the other two directions, an effect which was not found in the laboratory-prepared samples.

Structural anisotropy was also observed by Otte (1972a). Measurements on cement-treated crusher-run samples from 6 different freeway contracts indicated less anisotropy than recorded by Fossberg (1970). The dynamic elastic moduli in the direction of the compaction (called Modulus A) and perpendicular to this plane (called Modulus B) were recorded with an ultrasonic tester. The measurements were taken on wet and dry samples and the results are reported in Table 6.2.

TABLE 6.2 : Structural anisotropy in cement-treated crusher-run recovered from freeway contracts

CONTRACT	NO. OF SAMPLES TESTED	WET SAMPLES			DRY SAMPLES		
		Modulus A	Modulus B	Aniso-tropy	Modulus A	Modulus B	Aniso-tropy
1	6	34 600 (2,3)	37 000 (4,6)	1,069	25 100 (5,3)	28 700 (3,1)	1,143
2	12	30 100 (4,0)	35 900 (4,3)	1,192	23 200 (14,5)	27 800 (11,2)	1,198
3	12	25 200 (6,5)	29 200 (7,4)	1,158	17 300 (13,5)	19 500 (12,0)	1,127
4	12	29 700 (6,3)	31 900 (6,6)	1,074	20 700 (7,7)	23 900 (11,9)	1,154
5	9	27 444 (7,2)	30 178 (5,5)	1,099	23 666 (7,2)	27 266 (5,8)	1,152
6	10	29 000 (5,0)	32 200 (3,6)	1,110	25 000 (4,2)	30 400 (3,3)	1,216

The numbers in brackets are the coefficients of variation in per cent.

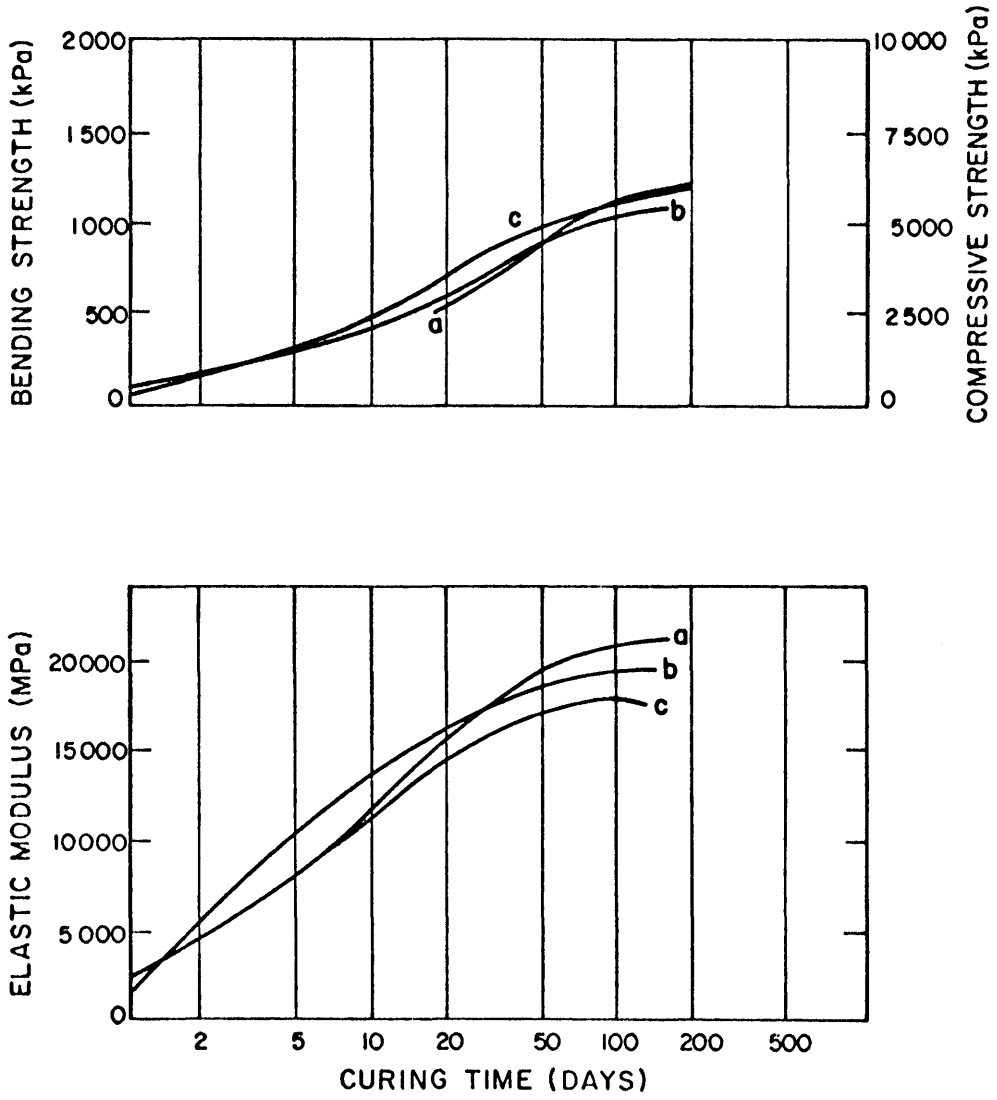

a = TRUCK MIXING AND FIELD COMPACTION
b = TRUCK MIXING AND LABORATORY COMPACTION
c = LABORATORY MIXING AND COMPACTION

FIGURE 6-1

EFFECT OF MIXING AND COMPACTION ON ELASTIC PROPERTIES OF A SOIL-CEMENT (after Fossberg 1970)

Anisotropy is real and it can affect the relationship between field- and laboratory-prepared samples since the outcome of the comparison depends on the direction in which the properties of the field samples were determined.

The results of a previous study (Otte, 1974) indicated a strong possibility that the construction technique has a significant influence on the properties of cement-treated materials. Samples were taken from fourteen pavements which were built by different contractors and supervised by various authorities and consulting engineers. Although all the contracts were constructed to the same nominal specification and thus regarded by engineers to be of the same quality, the differences in the material properties were significant. The bending strength varied between about 400 and 4 400 kPa, that is a factor of 10; the strain at break varied between about 113 and 251 με, a factor of 2,2; and the elastic modulus varied by a factor of 10,5 between about 3 700 and 38 900 MPa. These results indicate that cement-treated materials should not be regarded as having the same structural capacity just because they were built to the same specification.

On two adjoining cement-treated crusher-run sections, described in section 3.2.1.1 (page 39), the material quality differed significantly. Although the same material, specification and construction team applied to both, the one had a high elastic modulus and was cracked while the other one had a low elastic modulus and was uncracked. This significant difference in materials quality could really only have been caused by the construction variations.

The literature survey seems to indicate that the important parameters to ensure reasonable agreement between field- and laboratory-prepared samples are (i) cement content and the uniformity of its distribution, (ii) density, (iii) delay between mixing and compaction, and (iv) efficient curing. If good agreement between the field and laboratory conditions can be maintained for these parameters, the material properties ought to agree also.

6.3 DESCRIPTION OF CONTRACTS

A brief description and location of the 10 contracts evaluated in the study are given in Table 6.3. It contains the road number, the layer thickness, the maximum dry density at Mod. AASHO compaction and the optimum moisture content of the untreated soil, the average field density of the material, the approximate construction date, and the use of the material in the structural layout.

TABLE 6.3 : Description of the contracts sampled for a study of field versus laboratory properties of cement-treated materials

CONTRACT NO.	ROAD NUMBER AND LOCATION	LAYER THICKNESS (mm)	MAXIMUM DRY DENSITY (kg/m^3)	OPTIMUM MOISTURE CONTENT (%)	AVERAGE FIELD DENSITY (%)	CONSTRUCTION DATE	LAYER
1	Residential streets in Lynnwood Glen	150 150 150	1 838 1 770 1 833	17,3 20,5 16,5	95 95 96	November and December 1975	Subbase
2	S-12, Argent to Kendal	150 150 150	2 140 2 140 2 160	7,1 7,1 7,0	96 97 97	February and March 1976	Lower subbase Upper subbase Lower subbase
3	P158/2, Diepsloot to Mnandi	150	2 020	10,1	97	7 April 1976	Subbase
4	P56/2, Vergenoeg to Vaal River	150	1 935	12,4	95	20 April 1976	Subbase
5	Apron at Jan Smuts Airport	120	1 965	14,4	97	9 December 1975	Base
6	P88/1, Vereeniging	150	2 160	7,5	98	17 June 1976	Subbase
7	P106/1, Pretoria North	150	1 960	9	96	29 April 1976	Base
8	N1/23, Pienaars River to Warmbaths	150	2 030	13,6	95	26 May 1976	Lower selected subgrade
9	P5/1, Kinross	150	2 200	9	96	18 May 1976	Subbase
10	P73/1, Evaton	150	1 865	15,0	96	7 May 1976	Subbase

Contract 2 consisted of a number of experimental sections. In this study each experimental section was considered individually and they will be referred to by their S-numbers (NITRR, 1973) as for example 2(S6) or 2(S10). The third material mentioned under contract 2 is a lateritic soil that was used on sections 2(S7) and 2(S8). The first two materials are grindstone that was used on the other sections of the contract but the percentage compaction and the stabilizing agent (see later) were varied for the upper and lower subbase.

The reasons for stabilizing the various materials varied. This explains why the type of stabilizer and specified strength criteria varied. Table 6.4 summarizes the percentage and type of stabilizer used and the criteria aimed for.

TABLE 6.4 : Percentage and type of stabilizer and criteria

CONTRACT NO.	PERCENTAGE OF STABILIZER	TYPE OF STABILIZER	SPECIFIED STRENGTH CRITERIA
1	3 to 3,5	Lime	Reduction of plasticity index; did not aim for increased strength
2	3,75 4,0 5	50-50 mixture of Slagment and Portland cement	UCS*= 1 200 kPa after 7 days UCS*= 1 725 kPa " " " UCS*= 1 500 kPa " " "
3	3,5	Portland blast furnace cement	UCS*= 1 500 kPa after 7 days
4	4	Lime	CBR > 70
5	4	Lime	CBR > 70
6	4	Portland blast furnace cement	UCS*= 1 500 kPa after 7 days
7	4	50-50 mixture of Slagment and Portland cement	UCS*= 1 500 kPa after 7 days
8	3	50-50 mixture of Slagment and lime	Reduction of plasticity index; did not aim for increased strength
9	4	50-50 mixture of Slagment and lime	CBR > 160; laboratory values were around 180 to 200
10	4	50-50 mixture of Slagment and lime	CBR > 160; laboratory values on 7 samples were 174, 167, 201, 163, 154, 191 and 146
*UCS = Unconfined compressive strength			

On all the contracts the mix-in-place technique was used with disc harrows and motorgraders to do the mixing. The materials were usually compacted with grid rollers. After compaction the layers were usually kept moist for about 7 days, but if it was possible the tar prime coat was applied sooner. On contract 2 it was a condition of the contract that the curing membrane should be applied immediately after the final compaction or very early the next morning.

6.4 OUTLINE OF STUDY

After arrangements with the client, through the consulting engineer, the site was visited and block samples (about 600 x 600 mm) were sawn from the treated pavement layer. This was done somewhere between 7 and 27 days after construction of the layer but usually between 20 and 27 days after construction. On one or two contracts it was necessary to remove the blocks relatively early and they were slightly moistened, sealed in plastic and stored in a humid room at about 20 ^{o}C. About 27 days after construction the blocks were sawn into 6 or 7 beam samples (75 x 75 x 450 mm), allowed to soak in water for about 24 hours, and tested in flexure according to the procedure outlined in section 2.2.8(c). In this chapter these samples will be referred to as field samples.

Usually more than one block was removed from a particular section. This was necessary to cope with possible collapsing of the blocks during subsequent handling. From some sections it was possible to recover blocks, but it was not possible to saw them into beams because (i) the block had a fine crack which only showed up when it was sawn, or (ii) the matrix was too weak to hold the larger (+75 mm) stones and when sawn they pulled out and the beams crumbled, or (iii) the material was too soft under wet cutting with a diamond blade. If any of these failures occurred it was not possible to obtain field samples.

During a visit to a site a 40 kg sample of the untreated soil and a sample of the stabilizing agent actually used by the contractor were obtained. The relevant soil constants, such as maximum dry density and optimum moisture content, for the material used on the contract were also obtained from the site office.

These soil constants were used throughout the study and no checks were made on the properties of the particular soil sample. It is appreciated that some variations can occur, but it was considered a just representation of construction practice. From each soil sample, that is for each contract, 8 beam samples (75 x 75 x 450 mm) were made. The

samples were compacted for about 3 to 4 minutes on a table vibrating at 50 Hz, but the soil had to be placed in about 3 or 4 equal layers with tamping in order to work the predetermined mass into the mould. The samples were cured in a 100 per cent relative humidity room and tested at the same age as the corresponding field samples, which was usually 28 days. Hereafter these will be referred to as the laboratory-prepared samples.

Throughout the study it was endeavoured to compact the beams to the average density and percentage compaction measured by the resident engineer when he approved the construction of the layer. The differences between the materials on which soil constants were determined and those from which the samples were taken to prepare the laboratory specimens, and the difference between the specified optimum moisture content and that required by the vibrating compaction technique used in this study, did however result in lower densities being achieved in the laboratory (Table 6.5).

TABLE 6.5 : Difference in field and laboratory densities

CONTRACT	MAXIMUM DRY DENSITY OF MATERIAL (kg/m^3) (see Table 6.3)	FIELD SAMPLES		LABORATORY SAMPLES	
		Density (kg/m^3)	Percentage relative compaction	Density (kg/m^3)	Percentage relative compaction
1	1 770 to 1 838	*	-	-	-
2	2 140 2 140 2 160	2 064(2,2) 2 120(2,2) 2 083(5,9)	96 99 96	1 941(1,4) 1 954(1,8) 1 931(1,8)	91 91 89
3	2 020	1 968(0,1)	97	1 917(1,1)	95
4	1 935	*	-	1 777(1,8)	92
5	1 965	*	-	1 732(2,0)	88
6	2 160	*	-	1 960(1,1)	91
7	1 960	2 009(4,5)	102,5	1 803(2,2)	92
8	2 030	*	-	1 876(1,0)	92
9	2 200	2 114(3,3)	96	1 968(0,8)	89
10	1 865	*	-	1 712(1,2)	92

Numbers in brackets are the coefficient of variation in per cent.
*No field samples could be obtained; see 6.4

The averages and coefficients of variation of the 6 or 7 beams sawn from the field samples and those prepared in the laboratory, were calculated. For each contract the corresponding bending strengths, strains at break and elastic moduli in bending were compared.

6.5 RESULTS

The information obtained from the different contracts can be presented in various ways and it is possible to make various interesting observations.

6.5.1 Variation during a day's work

On five sections it was possible to saw beam samples from at least two different blocks. Since these blocks were constructed on the same day as part of the same section, the variations in their properties will indicate the variation during a day's work.

The contractor worked some of the adjoining experimental sections on contract 2 on the same day and although they are considered as separate contracts in this study, their variations may also be considered as variation during a day's work. They may therefore be included under this heading.

Table 6.6 contains the results and it appears that there was very little variation during a day's work. Statistically significant differences, at the 1 per cent level of significance, were only calculated for the bending strength and strain at break on contract 3, the elastic modulus on sections S5 and S6 of contract 2, and the bending strength between 2 of the 3 samples on contract 7. This implies that a section constructed on a particular day may be taken as homogeneous.

6.5.2 Variation in work performed on different days

Samples were recovered from the lower 150 mm of the cement-treated subbase on five sections of contract 2. These were all constructed with the same material and by the same construction team, but on different days. Table 6.7 shows the variations in material properties.

Engineers would normally regard these materials (Table 6.7) as having the same properties and structural capacity, because they were all constructed of the same materials, by the same contractor and according to the same specifications. A closer study of Table 6.7 will reveal that this assumption is incorrect since the bending strength varied by a factor of about 3,3, the strain at break varied by about 1,9 times, and the elastic modulus varied 2,3 times. Materials exhibiting these orders of variation should not be regarded as of the same quality!

TABLE 6.6 : Variation during a day's work

CONTRACT	NUMBER OF BEAM SAMPLES	BENDING STRENGTH (kPa)	STRAIN AT BREAK (με)	ELASTIC MODULUS (MPa)
2(S7)	8	785 (11,4)	129 (11,2)	7 788 (7,7)
	7	917 (21,4)	141 (13,2)	8 450 (8,7)
2(S8)	5	782 (18,4)	116 (15,4)	8 500 (4,3)
	7	785 (26,4)	130 (12,4)	7 992 (16,1)
3	6	502 (13,2)*	124 (16,4)*	5 900 (4,5)
	5	345 (7,1)	92 (14,5)	5 460 (2,1)
7	7	464 (17,3)*	237 (17,6)	2 825 (9,6)
	7	362 (17,1)	231 (27,4)	2 550 (17,1)
	6	385 (31,3)	249 (22,1)	2 608 (12,5)
9	5	129 (35,0)	172 (27,3)	1 810 (41,0)
	5	192 (37,3)	196 (20,1)	2 570 (28,5)
	6	173 (36,5)	225 (29,1)	2 190 (25,0)
2(S3)	6	843 (10,1)	92 (7,2)	10 683 (9,9)
2(S4)	7	928 (20,0)	89 (17,3)	11 264 (11,5)
2(S5)	5	632 (34,1)	128 (22,1)	6 199 (27,2)*
2(S6)	7	762 (19,2)	120 (11,4)	8 564 (12,3)
2(S16)	8	826 (20,9)	111 (17,3)	9 525 (15,1)
2(S17)	8	854 (16,3)	100 (16,0)	11 100 (18,7)

*Statistically significant variation at the 1 per cent level of significance.
The numbers in brackets are the coefficients of variation in per cent

TABLE 6.7 : Variation in quality of work performed on different days

CONTRACT	NUMBER OF BEAM SAMPLES	BENDING STRENGTH (kPa)	STRAIN AT BREAK (με)	ELASTIC MODULUS (MPa)
2(S3)	6	367 (35,7)	70 (7,5)	7 033 (24,5)
2(S6)	9	938 (12,5)	130 (15,0)	9 005 (7,6)
2(S10)	10	1 035 (24,1)	99 (13,0)	11 996 (13,3)
2(S17)	4	762 (11,1)	102 (26,1)	9 937 (20,0)
2(S19)	5	1 216 (24,0)	100 (17,1)	16 240 (2,5)

Numbers in brackets are the coefficients of variation in per cent

6.5.3 Variation within a layer

On two sections of contract 2 (sections S20 and S21) it was possible to saw and divide the blocks recovered from the lower 150 mm of the cement-treated subbase in such a way that beams could be sawn from both the upper and lower 75 mm of the layer. These will be referred to as the upper and lower halves respectively. The results are reported in Table 6.8.

TABLE 6.8 : Variation within a layer

CONTRACT	POSITION	NO. OF SAMPLES	BENDING STRENGTH (kPa)	STRAIN AT BREAK (με)	ELASTIC MODULUS (MPa)
2(S20)	upper	6	320 (16,0)	94 (18,3)	4 925 (24)
	lower	6	245 (17,0)	96 (16,1)	3 308 (15,3)
2(S21)	upper	5	361 (13,0)	104 (23,0)	5 600 (38,5)
	lower	5	162 (17,1)	120 (14,0)	2 590 (44,2)
The numbers in brackets are the coefficient of variation in per cent					

The student's t-test, at a 1 per cent level of significance, showed the difference in bending strength between the upper and lower halves to be significant for both the contracts. The differences in the strain at break were not significant. The elastic moduli for contract 2(S20) were significantly different at a 1 per cent level but on contract 2(S21) the difference was only significant at a 5 per cent level of significance.

From this study it may be concluded that on both contracts, although they were constructed on the same day, the upper half had both a higher bending strength and a higher elastic modulus than the lower half of the cement-treated layer.

6.5.4 Variation between field- and laboratory-prepared materials

Practical problems when sawing beams from the recovered blocks or during the laboratory preparation of the samples, resulted in only 4 contracts yielding information that can be utilized to compare field- and laboratory-prepared materials. This information is summarized in Table 6.9.

The table indicates that the properties of the field samples are generally lower than those of the laboratory samples. This does not, however, apply to contract 5, but this is probably due to the low density achieved in the laboratory. If generally higher densities could have been obtained in the laboratory, the differences between the field and laboratory samples may have been greater.

TABLE 6.9 : Variation in field- and laboratory-prepared materials

CONTRACT	FIELD-PREPARED			LABORATORY-PREPARED		
	Bending strength (kPa)	Strain at break (με)	Elastic modulus (MPa)	Bending strength (kPa)	Strain at break (με)	Elastic modulus (MPa)
2	Results were reported in Tables 6.6 and 6.7			817(13,0) 862(15,1) 753(22,0)	111(11,2) 106(7,1) 116(23,2)	10 625(10,0) 11 475(3,6) 9 417(3,4)
3	502(13,2) 345(7,1)	124(16,4) 92(14,5)	5 900(4,5) 5 460(2,1)	443(21,1)	97(11,0)	7 080(25,0)
5	221(49,5)	122(22,2)	2 750(19,1)	73(48,0)	86(28,0)	1 535(13,4)
6	Too many large stones in block; could not be sawn.			481(5,0)	101(13,2)	9 380(23,1)
7	464(17,3) 362(17,1) 385(31,3)	237(17,6) 231(27,4) 249(22,1)	2 825(9,6) 2 550(17,1) 2 608(12,5)	462(23,3)	138(25,0)	4 422(21,0)
8	Block too weak to resist the action of the blade when beams were cut			619(18,3)	189(16,0)	4 586(8,0)
9	129(35,0) 192(37,3) 173(36,5)	172(27,3) 196(20,1) 225(29,1)	1 810(41,0) 2 570(28,5) 2 190(25,0)	777(9,1)	161(7,6)	7 149(6,4)
The numbers in brackets are the coefficient of variation in per cent						

Comparing the results from contracts 7 and 8 makes interesting reading. The specified and required strength for contract 7 was 1 500 kPa while contract 8 was treated only to reduce the plasticity. This difference was borne out by the field samples because the quality of the material from contract 7 was better than that from contract 8; for example it could at least withstand the action of the saw. Statistically speaking the quality of the laboratory-prepared samples from the two contracts was the same. This implies that the material on contract 8 could have been prepared to obtain a better-quality treated material in the field. The economics of such an improvement depend on the particular site, but it is believed that it would have been economical to utilize the full potential of the treated material.

6.5.5 Variation in compressive strength

After performing the bending test, 150 mm long samples were sawn from the ends of the beams and tested in compression, although this was not done for all the field samples. The compressive strengths and the ratio between

these are given in Table 6.10. The results indicate a significant difference between the field and laboratory samples, but gives no clear indication of which method produced the highest compressive strength.

TABLE 6.10 : Variation in compressive strength of field- and laboratory-prepared materials

CONTRACT	FIELD SAMPLES (kPa)	LABORATORY SAMPLES (kPa)	RATIO
2	4 290(33,2) 6 367(22,0) 2 128(63,0)	2 443(6,7) 2 340(10,2) 4 050(13,1)	1,75 2,72 0,52
3	1 210(21,4)	1 830(9,1)	0,66
4	-	432(16,0)	-
5	-	488(28,2)	-
6	-	1 353(14,2)	-
7	2 303(28,3)	2 195(27,2)	1,05
8	282(28,4)	2 286(12,1)	0,12
9	917(42,1)	2 203(9,2)	0,42
10	559(32,1)	293(102,5)	1,91
Numbers in brackets are coefficient of variation in per cent			

6.6 DISCUSSION

The samples recovered from the various contracts indicated very little variation across a section constructed on a particular day (Table 6.6), but significant variations occurred across sections constructed on different days, that is at different occasions (Table 6.7). This implies that a specific section, constructed in one operation, may be considered homogeneous. However, different sections of a contract which were constructed on different days, may not be regarded as the same and the completed contract may therefore not be regarded as homogeneous. Neither may a layer be accepted as homogeneous in the vertical direction, since the upper part seems to have better material properties than the lower part.

The study of the difference between field- and laboratory-prepared samples generally indicated better material properties in the laboratory-prepared samples. This was to be expected since they were prepared under ideal conditions. The lower values for the field samples indicate that because of the construction technique, the full potential of the materials is not being utilized. Some research and development on construction techniques and procedures may therefore prove worthwhile.

The difference in material properties between the field- and laboratory-prepared materials, is an even more important consideration when the future application and implementation of a structural pavement design procedure based on layered elastic theory is considered. In the past an unconfined compressive strength has been specified as a materials requirement and the construction controls were a method specification together with a check on the specified compressive strength and density. If the contractor complied with these specifications the materials fitted into the original design definitions and the structural pavement design aspect virtually took care of itself, since it was an empirically developed procedure based on successful previous applications of this structural layout with this type of material. When applying the principle of balanced pavement design and layered elastic theory, it is important to know exactly the properties of the materials in the structural layout, and therefore to know to what extent the contractor can produce the quality of the laboratory-prepared samples. To utilize the materials and structural layout fully, the designer must know the amount of reduction he should allow for the difference between the laboratory and field values - this is the factor of safety in material properties. Not enough information is available in Table 6.9 to indicate the amount of reduction that should be allowed and more study on many more contracts will be required to obtain these numbers. In the meantime it seems that the field bending strength is somewhere between 20 and 150 per cent of the laboratory bending strength. The corresponding numbers for the strain at break and elastic modulus are between 63 and 180 and somewhere between 25 and 150 per cent respectively.

6.7 CONCLUSIONS

(a) Variation in material properties on a project as a result of the construction process is real and very significant. Pavement designers should take cognizance of this and somehow include it during the design stages.

(b) From the limited number of samples taken on a contract and the limited number of contracts suitable for this study it appears that:

  (i) The variation in material properties in a section constructed during a particular day is not significant and for pavement design purposes the section may be regarded as homogeneous.

(ii) The variation in material properties in sections constructed on different occasions or days is significant and these sections may not be considered the same, even when the same materials, contractor and specification apply to all the sections.

(iii) The material properties are not constant throughout the depth of the layer and the upper half seems to have higher values than the lower half.

(iv) The properties of materials constructed on a road by a contractor are significantly poorer than the values obtained on similar materials prepared in a laboratory. From this study it is not possible to indicate the degree of this difference.

(c) To try to predict the future behaviour of a pavement from cement-treated material properties obtained in a laboratory test, appears to be misleading. The extent of the difference between the design properties and the properties of the material produced by the contractor is unknown and it seems to vary from contractor to contractor. Neither is the difference constant during the construction period since it varies from day to day. Until these differences have been studied and quantified accurately, for example by tightening up the specification on the standard deviation of materials quality, it seems a very difficult task to predict accurately the long-term behaviour of a pavement containing cement-treated materials.

6.8 RECOMMENDATION

Until more specific recommendations become available for practical pavement design work, it is recommended that the values of the properties of field-prepared cement-treated materials be taken as 70 per cent of those of laboratory-prepared materials. A 30 per cent reduction in the laboratory values is thus recommended.